Water quality performance of pervious concrete pavements

By

VALERIE LÓPEZ CARRASQUILLO

A thesis submitted in partial fulfillment of the requirements for the degree of

MASTER OF SCIENCE

IN

CIVIL ENGINEERING

(Environmental and Water Resources Engineering)

UNIVERSITY OF PUERTO RICO

MAYAGÜEZ CAMPUS

July 2016

Approved by:

______________________________ ______________________
Sangchul S. Hwang, Ph.D. Date
President, Graduate Committee

______________________________ ______________________
Omar I. Molina Bas, Ph.D. Date
Member, Graduate Committee

______________________________ ______________________
Felipe J. Acosta Costa, Ph.D. Date
Member, Graduate Committee

______________________________ ______________________
Elizabeth Vanacore, Ph.D. Date
Representative, Graduate School

______________________________ ______________________
Ismael Pagán Trinidad, MSCE Date
Chair, Department of Civil Engineering and Surveying

Abstract

Water is one of the most important resources for human needs and, in some countries, the lack of potable and drinking water is a serious issue. For this reason, new infrastructure that increases water conservation and improves water quality is necessary. Pervious pavement allows water to infiltrate through its matrix, providing an alternative for water collection and storage and, in many cases, removing pollutants from water.

Six different pervious concrete pavement (PCP) mixtures were tested for compressive strength, permeability, and most importantly pollutant removal. The first PCP specimen (Opt 1) had the ratios of liquid to binder (L/B) at 32%, fly ash to binder (FA/B) at 24%, nanoparticles to FA (NP/FA) at 1.9%, and water reducer to binder (WR/B) at 0.35%. The second PCP specimen (Opt 2) had a composition of 32% L/B, 26% FA/B, 0% NP/FA and 0.25% WR/B. The third PCP specimen (Opt 3) had 32% L/B, 0% FA/B, 1% NP/FA and 0.20% WR/B. The fourth PCP specimen (Opt 4) had 36% L/B, 35% FA/B, 6% NP/B and 1.20% WR/B. The fifth PCP specimen (Opt 5) had a composition of 50% L/B, 60% FA/B, 0.04% NP/B and 1.71M NaOH. The control PCP specimen (Ctrl) had 33% L/B with no other admixtures. The cement type General Use (GU) was used for Opt 1, Opt 2, Opt 3 and control, while for the Opt 4 and Opt 5 the cement type IP was used. Fly ash from a local coal-fueled power plant was used to replace part of the cement in the mixtures. The Opt 4 contained nano-iron oxide, while nano-silicon dioxide was incorporated in the Opt 1, Opt 3 and Opt 5. Water reducers were used from the Opt 1 to Opt 4, while the Opt 5 was alkali activated.

The average compressive strength of the Opt 1, Opt 2, Opt 3, Opt 4, Opt 5 and Ctrl was 17.2, 14.4, 10.5, 16.2, 4.7 and 9.6 MPa, respectively, whereas the average permeability was 8.1, 8.3, 12.6, 9.4, 5.0 and 15.0 mm/s, respectively. The PCP specimens were placed in cylindrical containers inside a rain simulation chamber. Infiltrating water through the PCP and the storage gravel layer was collected and tested for water quality. The results showed that the Opt 1, Opt 2, Opt 3, Opt 4 and the Ctrl had an average reduction of fecal coliforms by 100% and 93%, respectively. The average reductions of phosphate and nitrate for the all the specimens were 100% and 15%.

Resumen

El agua es uno de los recursos más importantes para los seres humanos y en algunos países la falta de agua potable es un grave problema. Por esta razón, se desea una nueva infraestructura que aumente la conservación del agua y la demanda de la calidad del agua. El pavimento permeable permite que el agua se infiltre a través de su matriz, proporcionando una alternativa para el recogido y almacenamiento de agua y en muchos casos la eliminación de contaminantes.

Seis diferentes mezclas de pavimento de concreto permeable (PCP por sus siglas en inglés) fueron analizadas en cuanto a resistencia a la compresión, la permeabilidad y más importante la eliminación de contaminantes. El primer espécimen de PCP (OPT 1) tenía las proporciones de 32% L/B, 24% FA/B, 1.9% NP/FA y 0.35% WR/B (Los factores mencionados están escritos por sus siglas en inglés). El segundo PCP (OPT 2) tenía una composición de 32% de L/B, 26% FA/B, 0% de NP/FA y 0.25% WR/B. La tercera muestra (OPT 3) tenía 32% de L/B, 0% FA/B, 1% NP/FA y 0.20% WR/B. El PCP cuarto (Opt 4) tenía 36% de L/B, 35% FA/B, 6% de NP/B y 1.20% WR/B. La muestra del PCP quinta (Opt 5) tenía una composición del 50% de L/B, 60% FA/B, 0.04% de NP/B y la concentración de NaOH 1.71M. El espécimen del control (Ctrl PCP) tenía 33% de L/B sin otros aditivos. El cemento tipo GU se utilizó para los Opt 1, Opt 2, Opt 3 y el control, mientras que para el Opt 4 y Opt 5 se utilizó del tipo de cemento IP. Cenizas volantes procedentes de una central eléctrica de carbón como combustible local, se utilizó para reemplazar parte del cemento en las mezclas. El Opt 4 poseía contenido de nano-partículas de óxido de hierro, mientras que la nano-partículas del dióxido de silicio fueron incorporadas en el Opt 1, Opt 3 y Opt 5. Los reductores de agua fueron utilizados desde el Opt 1 al Opt 4, mientras que el Opt 5 era alcalino activado.

La resistencia promedio de compresión del Opt 1 , Opt 2 , Opt 3 , Opt 4 , Opt 5 y Ctrl fue de 17.2, 14.4, 10.5, 16.2, 4.7 y 9.6 MPa , respectivamente, mientras que la permeabilidad promedio fue de 8.1, 8.3, 12.6, 9.4, 5.0 y 15.0 mm/s, respectivamente. Las muestras de PCP se colocaron en recipientes cilíndricos dentro de una cámara de simulación de lluvia. La infiltración de agua a través del PCP y la capa de grava de almacenamiento se recogieron y se probaron para la calidad del agua. Los resultados mostraron que el Opt 1, Opt 2, Opt 3, Opt 4 y el Ctrl tuvieron una reducción promedio de coliformes fecales por 100% y 93%, respectivamente. Las reducciones

medias de fosfato y nitrato para el Opt 1 fueron de 100% y 15%, respectivamente, mientras que para el Ctrl fueron 82% y 17%, respectivamente.

To all the people that believed in me.

To God for letting me get where I am.

To my parents and brother, for the support.

To Sammy, for being by my side.

Acknowledgements

One of the most important things for me is to be grateful, sometimes we can accomplish things on our own but without the HEDGE group, and I could not have reached my goal and the nickname Vee would not exist. I would like to thank HEDGE for opening their doors and letting me participate and contribute to science. I thank Prof. Sangchul Hwang for helping me to believe in myself, for always being at our side, and for being the best advisor I could have. I also want to thank my graduate committee members for professional services they have provided time during my study.

Victor and Amber, you are the best undergraduates I could have and I appreciate all the days and nights that you helped me with my project. Please do not change who you are, if so change only to improve. Linoshka! More than a partner you are a friend, I want to thank you and I appreciate you for sharing all your knowledge with me. Graduates students from the environmental laboratory! More than partners, you are my family. I want to let you know that you can count on me for anything you need.

Cynthia, Frances and Liliana, my sisters from another mom, you are my support, the people who I can trust. Thanks a lot for being there in the good and bad moments. I also want to thank some people who more than family are friends: my mom, dad, brother, boyfriend, sister in law and my niece.

Thanks to Essroc San Juan, Cemex, AES Puerto Rico, BASF, Grace chemical and Star Ready Mix for the support.

Table of Contents

List of Tables

List of Figures

List of Abbreviations & Acronyms

ANOVA - analysis of variants

CCD - central composite design

Ctrl - control

FA - fly ash

FA/B - fly ash to binder

FC - fecal coliform

L/B - liquid to binder

NP/B - nanoparticles to binder

NPS - non point source

Opt - Optimum

PC - pervious concrete

RSM - Response Surface Methodology

WR/B - water reducer to binder

Chapter 1: Introduction

1.1. Background and Justification

Water is one of humankind's most valuable resource. Water scarcity is a serious environmental threat and it is necessary to figure out how it can be resolved. Stormwater runoff from impervious pavement creates flooding and allows contaminants like car oil, fertilizer, and fecal coliform to flow into water resources nearby. Asphalt and conventional concrete are common construction material used for the impervious pavement. The problem could be fixed with pervious and porous pavements.

Porous concrete was used in the 80's, but it was until the World War II when it recognized with the name of Porous or Pervious Concrete (PC) (Patil et al., 2011). Once gained interest, it was compared with Conventional Concrete and the engineering community realized that PC had more benefits (McMillan, 2007). PC can control stormwater runoff by allowing runoff to pass through it (ACI, 2010). In addition, PC also improves water quality after infiltration and it can be used as water storage or contribute to groundwater recharge (EPA, 2015).

Reusing, reducing, and/or recycling materials is a useful way to reduce pollution by decreasing the amount of waste that could end up in landfills. Coal fly ash (FA), an industrial byproduct from coal-fueled power plants, is a material often used in the production of concrete. FA can reduce the amount of cement in a concrete mix, thus reducing the environmental impact from cement production. For example, approximately 600,000 metric tons of CO_2 are annually produced in Puerto Rico due to cement production (EPA, 2015). FA improves the workability of a fresh concrete mix and enhances its durability and mechanical properties in most cases, especially after 180 days of curing (Antoni et al., 2015).

However, it should be noted that dissimilar mix designs of PC create different compressive strength, permeability, and water quality enhancement. Therefore, pervious concrete pavements (PCPs) made of different mixtures must be evaluated for their structural strength, hydrologic property and water quality performance for successful implementation. A few factors to consider when implementing PC are the precipitation of the place and the purpose of application for either parking lot, sidewalk or road, among others. Then one can begin the design of it with the selection of appropriate construction materials, dimension of reservoir layers and underdrain structures, and the most importantly the mixture of PC.

1.2. Objectives

This project aimed to quantify water quality performance of several PCPs with dissimilar properties in terms of mix design and the type of admixtures. To meet this end, a lab-scale experiment was conducted to:

1. Make a Response Surface Methodology (RSM) to optimize the pervious concrete mix for the compressive strength and permeability,
2. Compare compressive strength, permeability and costs of six different mixes.
3. Assess the water quality performance of several PCP systems for removal of organic and anionic pollutants and fecal coliform (FC), and
4. Implement the best PCP mix at a field site.

Chapter 2: Literature Review

2.1. Cement

The most common cement is the Portland cement (PC), which is mostly composed of lime, silica fume and iron (Gagg, 2014). Portland cement is one the most valuable material for infrastructure development. Portland cement is categorized in different types, depending on its characteristics and uses, as shown in Table 1. Mindess et al. (2003) specify the typical composition of the Portland cement, as shown in Table 2.

Table 1. Characteristics of the different types of Portland cement (ASTM C150)

Type	Characteristics
I/IA*	For use when special properties specified for any other type are not required
II/IIA	For general use, more especially when moderate sulfate resistance is desired
II(MH)/II(MH)A	For general use, more especially when moderate heat of hydration and moderate sulfate resistance are desired
III/IIIA	For use when high early strength is desired
IV	For use when a low heat of hydration is desired
V	For use when high sulfate resistance is desired

***A:** cement containing air entraining admixture

Table 2. Chemical composition of Portland cement (Mindess et al., 2003)

Chemical Name	Chemical Formula	Notation	Weight Percentage
Tricalcium silicate	Ca_3SiO_5	C_3S	55 (37-71%)
Dicalcium silicate	Ca_2SiO_4	C_2S	18 (4-36%)
Tricalcium aluminate	$Ca_3Al_2O_6$	C_3A_2	10 (0-14%)
Tetracalcium alumino-ferrite	$Ca_4Al_2Fe_2O_{10}$	C_4AF	8 (4-19%)
Calcium sulfate dehydrate	$CaSO_4{\cdot}2H_2O$	CSH_2	6 (1-7%)

2.2. Fly Ash

The production of cement produces high amounts of CO_2, which is one of the greenhouse gases responsible for environmental pollution and global warming (Jo et al., 2014). Mineral admixtures such as FA, silica fume, and slag are used as partial substitute of the cement used in concrete (Jamal, 2014). FA is a byproduct of electricity production at coal-fueled power plants. The use of FA as partial substitute of cement resulted in improvement of mechanical properties of PC (Vázquez-Rivera et al., 2015). FA can be divided into two different categories: Class F and Class C. The difference between them is shown in Table 3.

Table 3. Chemical composition of FA types specified in ASTM C618

Chemical Composition (mass %)	**Class F**	**Class C**
$SiO_2 + Al_2O_3 + Fe_2O_3$	70.0 Min	50.0 Min
Sulfur Trioxide (SO_3)	5.0 Max	5.0 Max
Moisture Content	3.0 Max	3.0 Max
Loss on Ignition	6.0 Max	6.0 Max

2.3. Nanoparticles

During the past years, interest in nanotechnology application in cement and concrete has increased. Therefore, it is important to understand the effects of these nanomaterials on cement and concrete chemistry. Nanoparticles are nano-size microscopic materials, which are less than 200 nm in diameter (Amin and Abu el-hassan, 2015). The investigation of their effect on concrete has become a major study area over the past years (Mohamed, 2015). Some of the most used nanomaterials in concrete are nano-Fe_2O_3 and nano-SiO_3. Studies confirm that the use of nanoparticles increases the strength of concrete (Phoo-ngernkham et al., 2014).

2.4. Water Reducer

The water-cement ratio used in a concrete mixture affects the properties of resistance and workability. In order to increase the resistance of a concrete mixture, the lowest water-cement ratio possible should be used. Water reducers, also known as plasticizers, are used to reduce the amount of water in a concrete mix without compromising its workability, thus resulting in a structurally stronger concrete (Tkaczewska, 2014).

2.5. Stormwater Runoff

Stormwater runoff occurs when the rain is not infiltrated through the ground. In natural ground cover areas, approximately 50% of the rainfall infiltrates through the ground, while only 10% becomes runoff water (Figure 1). On the other hand, the water infiltration of high-density residential, industrial, or commercial areas is only 15%, increasing the amount of runoff water up to 55% (Hill, 2015).

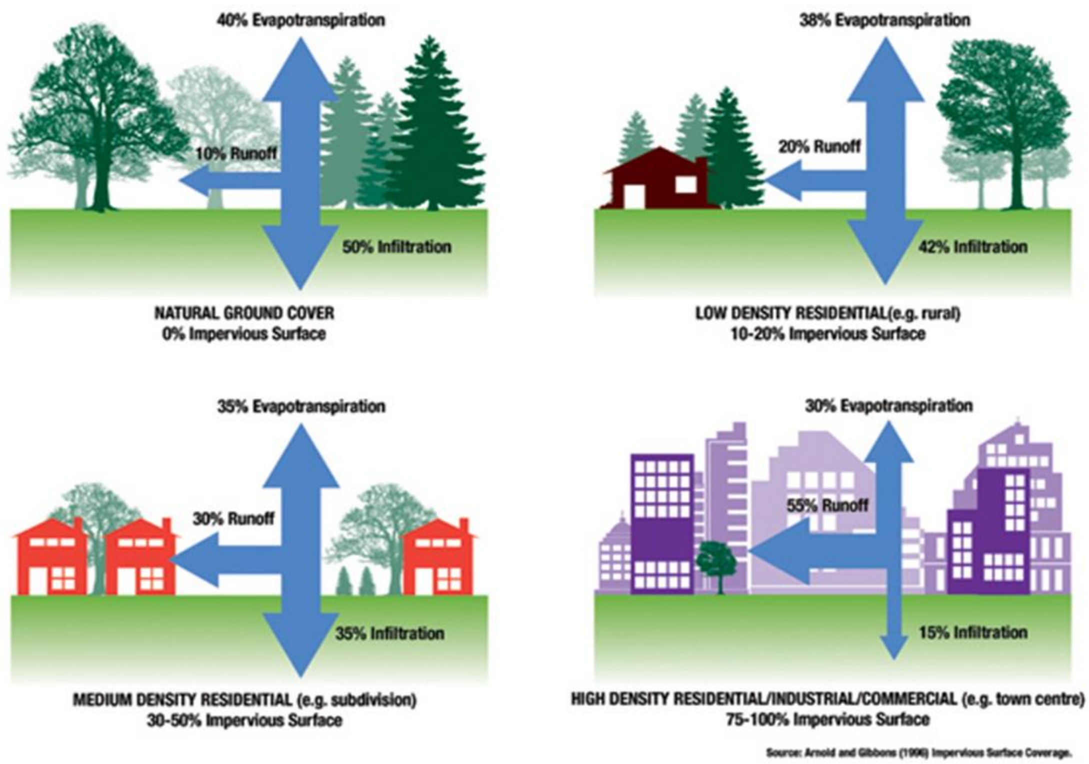

Figure 1. The effects of impervious surfaces on water infiltration and runoff (Hill, 2015)

Impervious grounds such as roads, sidewalks, parking lots, and rooftops are the main reason for both flooding and contaminant flow to water resources (EPA, 2012). Some of these pollutants are phosphorus, bacteria, oil, trash, pesticides, and metals. Managing the overall risk associated with the stormwater runoff in order to prevent its adverse effects is of great importance (Parker et al., 2010).

2.6. Non-Point Source (NPS) Pollution

NPS arises from stormwater runoff, atmospheric deposition, drainage, or seepage (EPA, 2016). Population growth increases the volume of wastewater, which simultaneously increases the amount of pollutants in water resources (Abdel-Raouf et al., 2012). Water runoff transports some pollutants through the flow on impervious surfaces. Some of these pollutants are automotive oil, fertilizers, sediments, and bacteria. The treatment of wastewater is imperative, as it is a risk to the environment and to public health (Asadollahfardi et al., 2016).

Water treatment is as important as water management because some countries suffer from lack of clean water and wastewater treatment (Abegunrin et al., 2016). An appropriate management control of NPS with an effective water treatment could achieve a functional water system.

2.7. Water Quality

The lack of clean water in some countries is a serious issue. It is important to assess water quality in order to quantify its physiochemical and biological characteristics and identify the appropriate treatment technology. One of the major problems of water quality is its contamination with high amounts of fertilizers caused by agricultural activity. Fertilizers contain high concentrations of phosphorus and nitrogen, which cause eutrophication in water resources (Irmedez et al., 2006). Eutrophication is an increase of algae growth as a response of a high amount of nutrients, which can cause the depletion of oxygen in water and consequently the death of fish and shellfish in water resources.

Pathogenic bacteria that are often present in stormwater runoff negatively affect public health (Parker et al., 2010). Fecal coliforms (FC) are indicator microorganisms for the pathogens that would come from warm-blooded animals including humans. In other words, the presence of FC indicates the presence of other harmful microorganisms in water resources (Luck et al., 2009). Agro-industrial farms near water resources are of big concern to public health since they are potential sources of harmful microorganisms (Soller et al., 2015).

2.8. Pervious Concrete Pavement

As population is increasing, a greater fraction of land becomes impervious (Nguyen et al., 2014). Pervious concrete (PC) is new in the industry, and has been used for the construction of green and sustainable rooftops or pavements. The PC can mitigate runoff water, improve the quality of water, can be used as water storage, contributes to groundwater recharge, and allows air and water to reach tree roots (ACI, 2010). Pervious concrete pavement (PCP) also conserves soil moisture underneath the pavement and absorbs vehicle noises (Yang and Jiang, 2003). Some of the disadvantages of the use of pervious pavements, when not correctly installed, include the risk of clogging and a limitation in its durability and strength (Zhong and Wille, 2015).

The PC can be made of a coarse aggregate, cement, water, and admixtures. It usually contains a void content of 15 to 25%, a thickness of 4 to 8 inches, a compressive strength of 2.8 to 28 MPa and a permeability of 10 feet/day (TDEC, 2014). PCPs are made of a filter layer, underdrain, and reservoir and bedding layer.

2.9. Response Surface Methodology (RSM)

Response Surface Methodology (RSM) is used in the development of a relationship between the responses of interest and the variables denoted (Khuri and Mukhopadhyay, 2010). The objective of RSM is to optimize the response or target a specific response (Montgomery, 2013). RSM was made in Minitab 17. Central composite design (CCD) has been the most commonly used design method with RSM in statistically assessing the mathematical relationship between the independent variables and the responses. The CCD was used to estimate first and second terms and model a response variable with a curvature (Minitab, 2015).

CCD involves the use of a two-level of full or fractional factorial points (16 points for a 4 factor design (i.e., k=4)), *2k* axial points, and center points. The number of center points depends on the replication. CCD can have different design properties by controlling the value of α that is the distance from each axial point to the center of the design space. A more common choice of α is $\alpha = k^{1/2}$ or $\alpha = (N_F)^{1/4}$, where N_F is the number of factorial points in a k factor design. The factorial points contribute to the estimation of the interaction terms. The center points provide information about the existence of curvature in the system, with which the axial points allow to estimate the quadratic terms.

Chapter 3: Design and optimization of PC mix by RSM

An RSM of 30 different specimens was made to optimize the pervious concrete mix for the compressive strength and permeability.

3.1. Materials

3.1.1. Cement and Fly Ash

Portland cement that was used in this experiment was the type GU cement in compliance with the ASTM C1157. The FA used was from AES Puerto Rico, which is a local coal-fueled power plant. The chemical properties of these materials are shown in Table 4.

Table 4. Chemical composition IP and GU cements and FA

Property	IP Cement	GU Cement	Fly-Ash
SiO_2	27.14	19.8	30.84
Al_2O_3	6.68	5.1	9.93
Fe_2O_3	3.71	3.1	5.01
CaO	55.47	67.3	39.61
MgO	1.62	0.8	0.35
K_2O	0.48	-	1.01
Na_2O_3	0.59	-	0.9
SO_3	3.48	2.7	11.43
TiO_2	0.32	-	0.45
P_2O_5	0.11	-	0.11
Loss-on-ignition (wt.%)	5.52	6.8	7.62
Blaine (m^2/kg)	554	554	441
Fineness (wt.%)[a]	92.6	92.6	73.7

a Wet sieve percentage passing the No.325 (45μm) sieve (ASTM C430)

3.1.2. Nanoparticles and Coarse Aggregate

The nanoparticle used was nano-silica (SiO_2). Nano-SiO_2 is a white powder with an average diameter of 20 to 30 nm, and was acquired from US Research Nanomaterials (Houston, TX).

Limestone gravel in sizes of 4.75-12.5 mm was used to produce the PC. The gravel was purchased at a local hardware store. It was sieved, cleaned and dried prior to use.

3.2. Methodology

3.2.1. Samples Preparation

Minitab 17 created a two-level, four-factor central composite design. The program helped aid the process of designing different mixes and creating an optimum one. The factors considered were the weight percentages of FA, nano-SiO_2, water reducer, and water to binder. The factors and levels of the central composite design are shown in Table 5. The optimization aimed to produce the PC specimen having the highest compressive strength and a targeted permeability at 8 mm/s.

Table 5. RSM design of the two level, four factor central composite design

FACTORS	LEVELS				
	-α	**-1**	**Center**	**1**	**+α**
Fly Ash (FA/B)	10	20	30	40	50
Nano-Silicate (NS/FA)	0	1	2	3	4
Liquid (W/B)	30	31	32	33	34
Water Reducer (SP/B)	0	0.25	0.5	0.75	1

3.2.2. Permeability Test

The permeability was measured by quantifying the water flow passing through the specimens using the constant head method, modified from ASTM D2434 in order to meet the specifications of the experiment. The system shown in Figure 2 allowed measuring the permeability in mm/s with Equation (1).

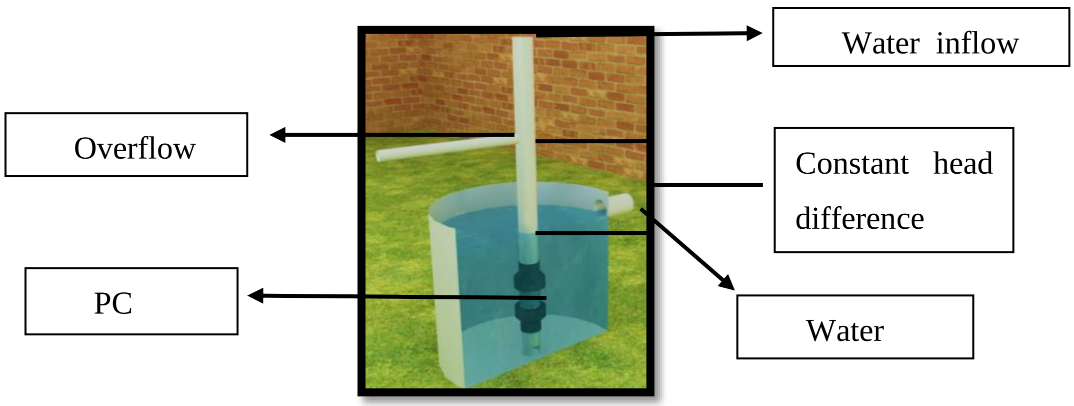

Figure 2. Permeameter

$$\textbf{Permeability} = \frac{4 \cdot V_w \cdot L}{\pi \cdot D^2 \cdot \Delta h \cdot t} \tag{1}$$

V_W- water volume at the time (t)

Δh- constant water head

D- diameter of the specimen

L- height of the specimen

3.2.3. Compressive Strength

The compressive strength of the PC specimens was measured after 28 days of curing, in accordance to the ASTM C39. Capping rubber pads (Gilson HM- 362) were positioned on the bottom and the top of the pervious concrete to obtain a uniform load during the breakup of the specimens. The machine used was a 3000-kN Forney universal testing machine that automatically records the load of failure. Figure 3 shows the machine used for the compressive strength test and how the specimen was placed.

Figure 3. Compressive strength testing

3.3. Results and Discussion

3.3.1. Response of the RSM

Table 6 shows the results from the testing of response variables of 30 different mixes in triplicate. The average compressive strength and permeability obtained ranged from 5.13 to 18.63 MPa and 0 to 17.61 mm/s, respectively.

Table 6. RSM results. Data shown are the average of triplicate specimens

Run Order	Independent variables (% wt.)				Dependent variables	
	FA/B	NS/FA	W/B	SP/B	Comp. Strength (MPa)	Permeability (mm/s)
1	30	2	32	0.5	18.51	6.50
2	40	1	33	0.25	12.87	10.49
3	40	1	31	0.75	9.02	0.00
4	40	3	33	0.75	12.94	0.00
5	20	1	33	0.75	10.91	0.00
6	20	3	33	0.25	18.60	9.52
7	20	1	31	0.25	16.40	11.28
8	40	3	31	0.25	3.39	14.96
9	30	2	32	0.5	19.34	6.86
10	20	3	31	0.75	12.31	0.00
11	40	3	31	0.75	8.96	10.68
12	20	1	31	0.75	7.64	0.00
13	40	1	31	0.25	7.66	15.36
14	40	1	33	0.75	7.70	0.00
15	20	3	31	0.25	13.04	13.18
16	30	2	32	0.5	15.08	0.00
17	30	2	32	0.5	13.20	8.30
18	20	3	33	0.75	12.13	0.00
19	40	3	33	0.25	5.13	16.42
20	20	1	33	0.25	13.85	11.86
21	30	0	32	0.5	12.32	0.00
22	10	2	32	0.5	8.94	0.00
23	30	2	32	0	8.70	16.91
24	50	2	32	0.5	6.96	17.61
25	30	2	32	0.5	18.63	7.74
26	30	4	32	0.5	12.89	12.82
27	30	2	30	0.5	12.15	16.75
28	30	2	32	1	5.49	0.00
29	30	2	34	0.5	12.90	3.52
30	30	2	32	0.5	15.46	7.71

A few specimens had a permeability at 0 mm/s. This was due to draindown of pastes because the mixture had an excess of water. Consequently, the bottom of the specimens was clogged as shown in Figure 4.

Figure 4. Clogged specimens due to draindown of the paste on the bottom

3.3.2. Contour Plots of the Response

A simple maximum pattern was observed for the compressive strength when the FA/B was in a function with NS/FA. The compressive strength was the highest near the center of the design from which the changes of FA/B and/or NS/FA decreased it (Figure 5A), with the charges of FA/B affecting slightly more than those of NS/FA. A similar pattern was observed for the factors of FA/B in the function of W/B (Figure 5B), and FA/B with SP/B (Figure 5C). The Figure 5D shown factors NS/FA and W/B are not affecting the compressive strength, instead the SP/B is affecting the compressive strength when the function are NS/FA and SP/B (Figure 5E), and W/B and SP/B (Figure 5F).

The permeability was increasing with decreasing of FA/B and NS/FA at the same time. The greatest permeability was obtained when both the FA/B and NS/FA were at highest levels (Figure 6A). Figure 6B was the inverse of Figure 6A in which the permeability was decreasing with increasing of W/B and SP/B. For the combinations of NS/FA and SP/B (Figure 6C) and NS/FA and W/B (Figure 6D) the highest permeability was obtained at the highest levels of NS/FA with the other factor being the lowest. On the other hand, the highest permeability was obtained at the highest level of FA/B with the lowest level of SP/B or W/B (Figures 6E and 6F).

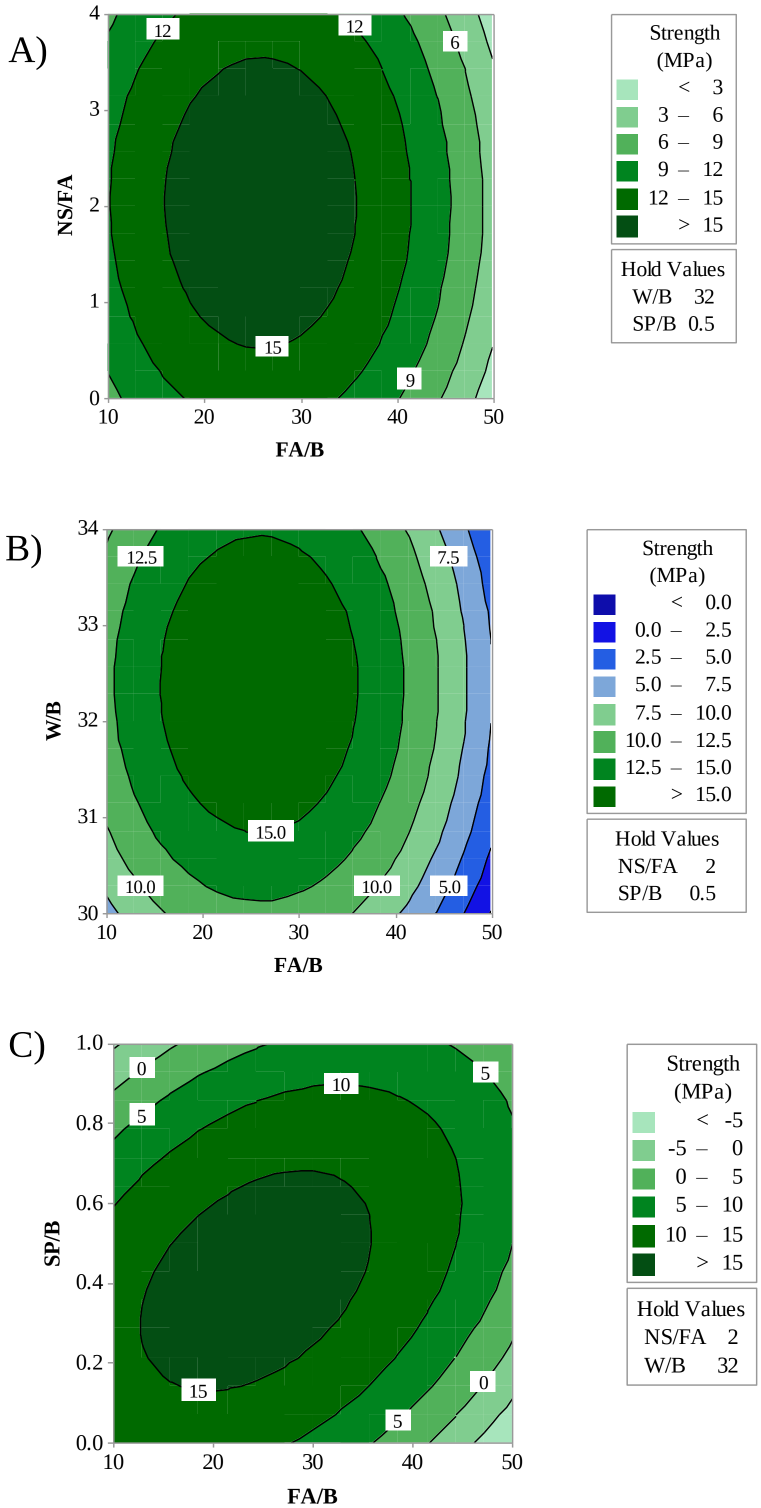

Figure 5. Contour plots of compressive strength for obtaining the best ratio

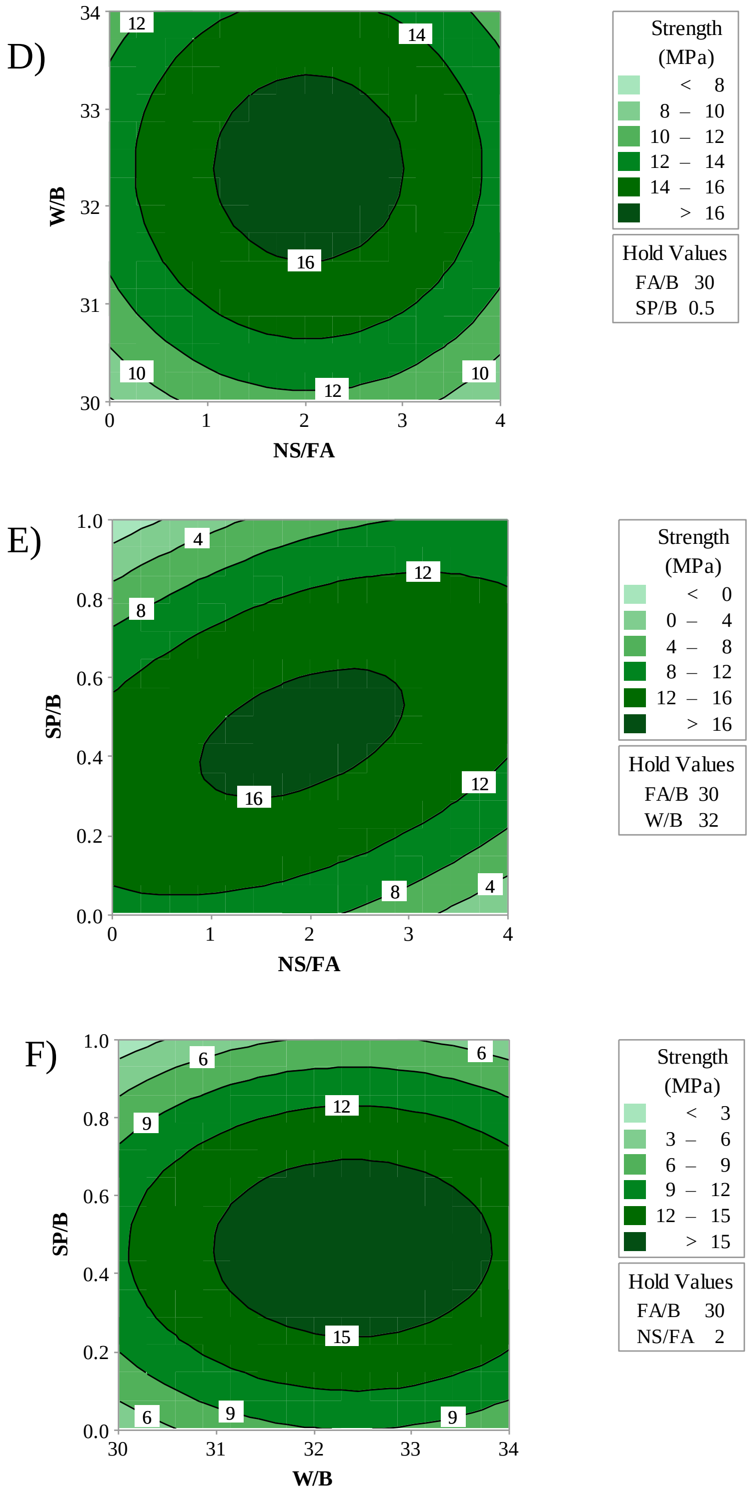

Figure 5. (Continued).

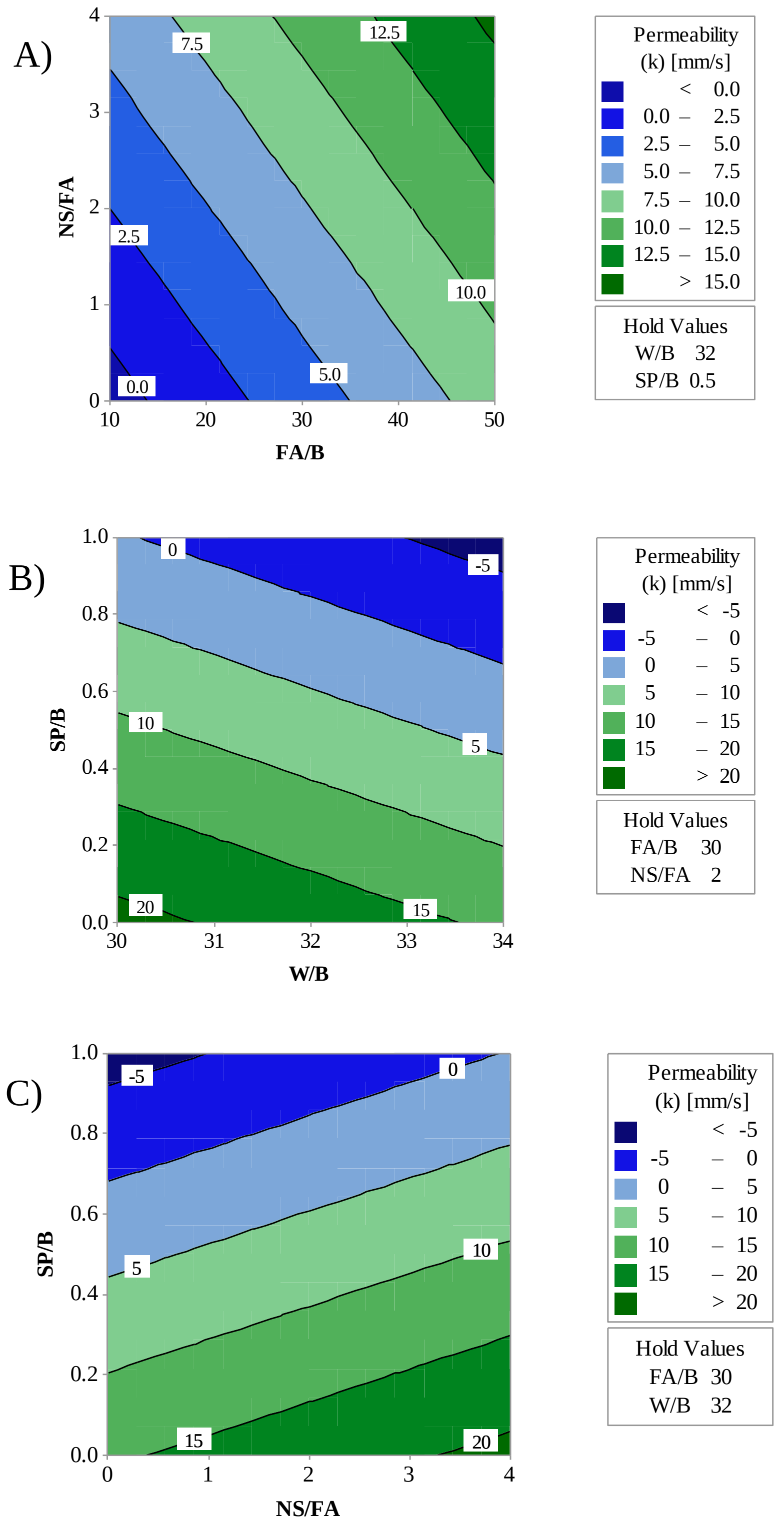

Figure 6. Contour plots of permeability for obtaining the best ratio

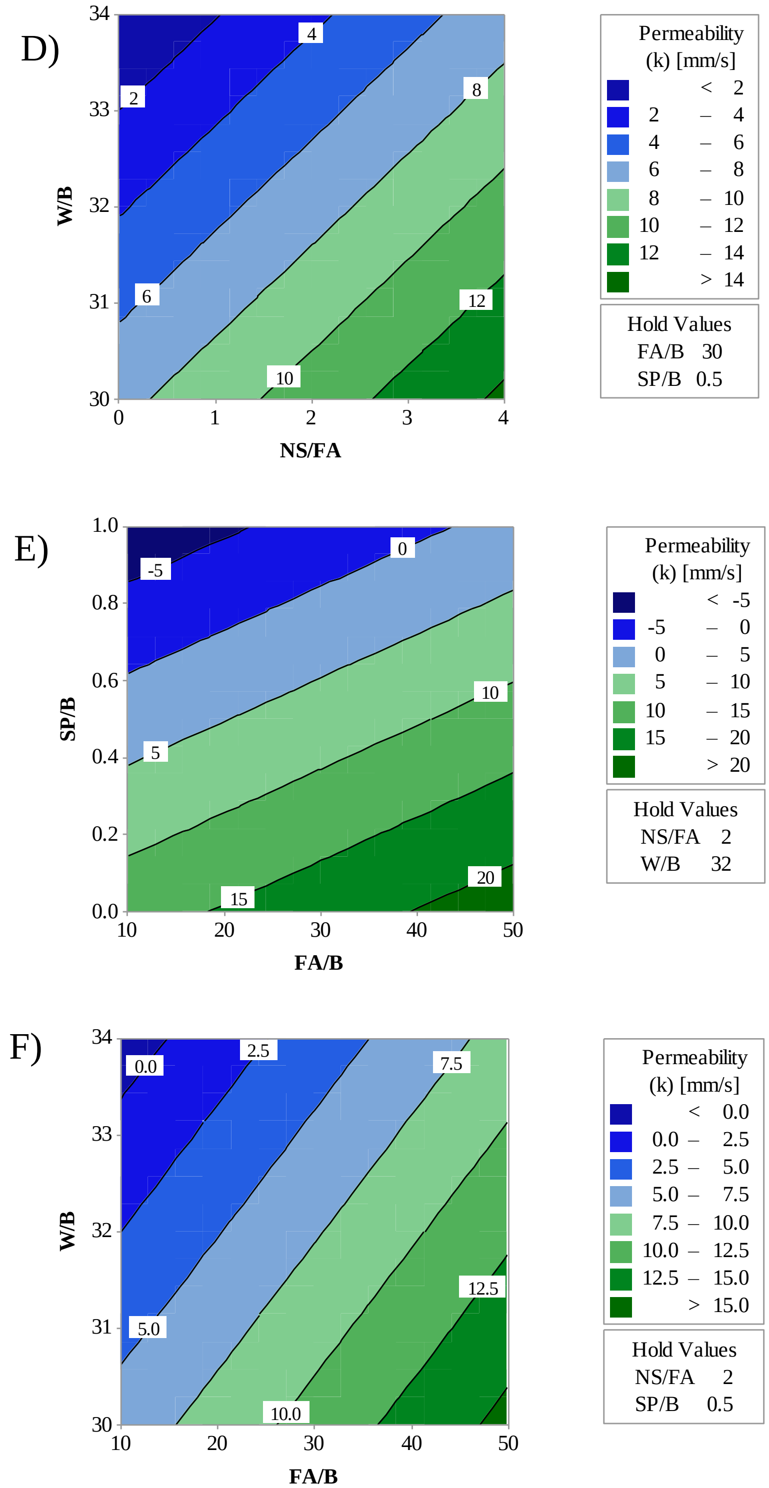

Figure 6. (Continued).

3.3.3. Optimum Mix

The last step was to determine the optimum mix and validate the results. Figure 7 shows the response optimizer of Minitab 17, in which the ratios of mix for the highest compressive strength and the target permeability are predicted simultaneously. In this case, the ratios obtained were 24 % FA/B, 1.90 % NS/FA, 32 % W/B and 0.35% SP/B for the compressive strength and permeability with 8.82 mm/s and 17.23 MPa, respectively. Table 7 shows part of the ANOVA with the significant values.

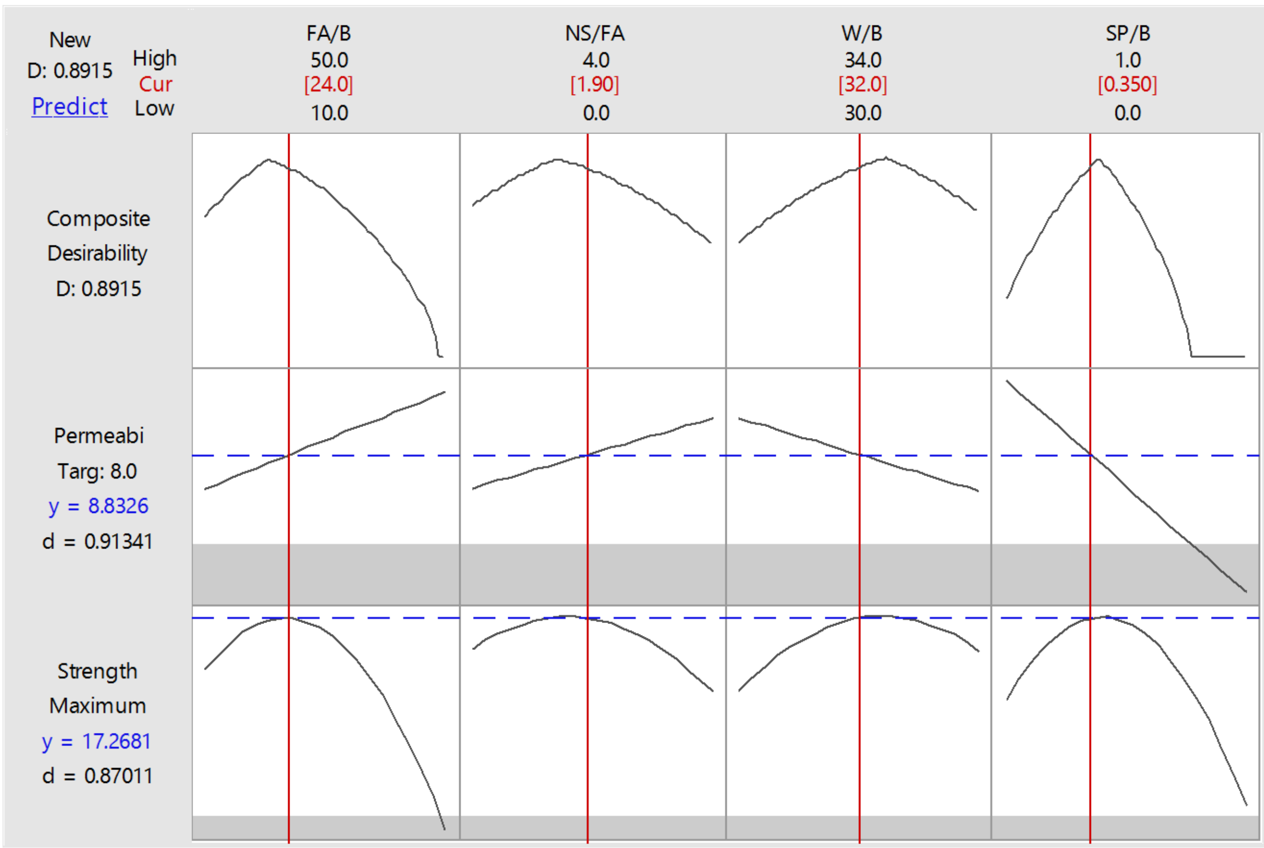

Figure 7. Response optimizer.

Table 7. p-values and coefficients of the factors

Term	Compressive Strength		Permeability	
	p-value	coefficient	p-value	coefficient
Constant		-958.000		65.300
FA/B	0.000	0.711	0.002	0.239
NS/FA	0.867	0.960	0.016	1.726
W/B	0.087	59.700	0.012	-1.817
SP/B	0.115	1.630	0.000	-21.030
$(FA/B)^2$	0.000	-0.021		-
$(NS/FA)^2$	0.026	-0.901		-
$(W/B)^2$	0.023	-0.921		-
$(SP/B)^2$	0.000	-36.450		-
FA/B*SP/B	0.002	0.712		-
NS/FA*SP/B	0.012	5.420		-
R^2 (%)		87.700		79.96
Lack of Fit	0.367		0.624	

The prediction models for permeability and compressive strength are shown in Eqs. (2) and (3), respectively. It should be noted that Eqs. (2) and (3) contain only those terms statistically significant ($p<0.05$) and that the coefficient values are for the uncoded terms:

$$\mathrm{Permeability\ (mm/s)} = 65.300 + 0.239 * \mathrm{FA/B} + 1.726 * \mathrm{NS/FA} - 1.817 * \mathrm{W/B} - 21.030 * \mathrm{SP/B} \tag{2}$$

$$\mathrm{Compressive\ Strength\ (MPa)} = -958 + 0.711 * \mathrm{FA/B} + 0.960 * \mathrm{NS/FA} + 59.700 * \mathrm{W/B} + 1.630 * \mathrm{SP/B} - 0.021 * (\mathrm{FA/B})\hat{}2 - 0.901 * (\mathrm{NS/FA})\hat{}2 - 0.921 * (\mathrm{W/B})\hat{}2 - 36.450 * (\mathrm{SP/B})\hat{}2 + 0.712 * \mathrm{FA/B} * \mathrm{SP/B} + 5.420 * \mathrm{NS/FA} * \mathrm{SP/B} \tag{3}$$

Chapter 4: Comparison of structural strengths, hydrologic properties, physical durability and costs of PC specimens

In this chapter, several PC specimens that were prepared with optimum mixes were compared with the strength, permeability, durability and production costs.

4.1. Materials

4.1.1. Cement and Fly Ash

The two types of Portland cement that were used in this experiment are type GU cement and type IP cement in compliance with the ASTM C1157. The FA was from AES Puerto Rico, which is a local coal-fueled power plant. The chemical properties of these materials are shown in Table 4 in Chapter 3.

4.1.2. Nanoparticles and Coarse Aggregate

The nanoparticles used were nano-silica (SiO_2) and nano-iron (Fe_3O_4). Nano-SiO_2 is a white powder with an average diameter of 20 to 30 nm, and was acquired from US Research Nanomaterials (Houston, TX). Nano-Fe_3O_4 used is a black liquid with a nominal size of 10 nm and was purchased from Ferrotec (Bedford, NH). The coarse aggregate used is the same of Chapter 3.

4.2. Methodology

4.2.1. Preparation of Different Optimum Specimens

Using Minitab 17, a central composite design was created. The program was a resourceful tool when designing different mixes and seeking the optimum ones. Six different PCP mixtures were tested for compressive strength, permeability, LA abrasion, and costs. The ratios of the mixes are in Table 8. The cement type GU was used for the Opt 1, Opt 2, Opt 3 and control, while for the Opt 4 and Opt 5 the cement type IP was used. The Opt 4 contained nano-iron oxide, while nano-silicon dioxide was incorporated in the Opt 1, Opt 3 and Opt 5. Water reducers were used from the Opt 1 to Opt 4, while the Opt 5 was alkali activated.

Table 8. Ratio of six different optimum PC mixes

FACTORS	**PCP**			
	Opt 1	**Opt 2**	**Opt 3**	**Ctrl**
Fly Ash (FA/B)	24	26	0	0
Nano-Silicate (NS/FA)	1.9	0	1	0
Liquid (W/B)	32	32	32	33
Water Reducer (SP/B)	0.35	0.25	0.20	0

FACTORS	**PCP**	**FACTORS**	**PCP**
	Opt 4		**Opt 5**
Fly Ash (FA/B)	35	Fly Ash (FA/B)	60
Nano-Iron (NI/B)	6	Nano-Silicate (NS/B)	0.04
Liquid (W/B)	36	NaOH (mole/L)	50
Water Reducer (SP/B)	1.2	Liquid (NaOH/B)	40

4.2.2. Permeability Test and Compressive Strength

The permeability test and compressive strength were tested in the same way as discussed in Chapter 3.

4.2.3. LA Abrasion Test

The ASTM C1747 was used for the Los Angeles Abrasion test to determine the resistance of the PC. The resistance can be known by measuring the mass loss using a rotating steel drum shown in Figure 8. The procedure for this test is the following according to the ASTM C1747; measure the weight and place the three specimens into the drum. Then rotate the machine at 50, 100, 150, 200, 250, 300, 350, 400, 450 and 500 revolutions for 10 min. It is important to record mass for all the revolutions. Also, one should discharge the material from the machine and hand sieve the material on a 25 mm sieve. The mass loss percentage was calculated with the differences between the original and final masses of the three specimens divided by the original mass multiplying 100% as shown in Equation 4.

$$\mathrm{M_{loss}}(\%) = \left(\frac{M_O - M_\mathrm{f}}{M_\mathrm{O}}\right) \times 100 \tag{4}$$

The experiment was made to compare four different mixes which were Opt 1, Opt 4, Opt 5 and Ctrl.

Figure 8. Los Angeles Abrasion machine

4.3. Results and Discussion

4.3.1. Compressive Strength, Permeability and Costs

Six different mixes were tested for compressive strength and permeability. Table 9 shows that the Opt 1 had higher compressive strength than the other mixes. Also it was found that permeability and cost ranges from 5 to 15 mm/s and \$271.22 to \$3,057.55 per yd^3, respectively. The lowest cost was found with the control because it did not have admixtures.

Table 9. Responses of six different optimum PC mixes

Sample	FA/B	NP/FA	L/B	SP/B	Average Strength, 28 days (psi)	Average Strength, 28 days (MPa)	Average Permeability (k) [mm/s]	Cost ($/yd^3)
Opt 1	24	1.9	32	0.35	2495	17.2	8.1	282.45
Opt 2	26	0	32	0.25	2088	14.4	8.3	277.98
Opt 3	0	1	32	0.20	1529	10.5	12.6	276.62
Ctrl	0	0	33	0	1389	9.6	15.0	271.22

Sample	FA/B	NP/B	L/B	SP/B	Average Strength, 28 days (psi)	Average Strength, 28 days (MPa)	Average Permeability (k) [mm/s]	Cost ($/yd^3)
Opt 4	35	6	36	1.20	2355	16.2	9.4	3,057.55

Sample	FA/B	NP/B	L/B	SP/B	Average Strength, 28 days (psi)	Average Strength, 28 days (MPa)	Average Permeability (k) [mm/s]	Cost ($/yd^3)
Opt 5	60	0.04	50	0	682	4.7	5.0	509.47

The 28-day compressive strength of six different mixes were ranged between 4.7 and 17.2 MPa, with the Opt 1 having the greatest followed by the Opt 4. Alkali-activated Opt 5 had the lowest 28-day compressive strength of all.

With respect to the permeability, the control specimen had the highest of all at 15.0 mm/s, whereas the Opt 5 had the lowest at 5.0 mm/s. In general, the higher compressive strength of the specimen was, the lower permeability was found, except for the Opt 5 that had the lowest testing valves in both compressive strength and permeability.

The optimum mixes and control that were developed in current study showed twice production costs (~\$280/yd^3) than the Opt 5 (~\$510/yd^3). The production cost of the Opt 4 was very high (~\$3000/ yd^3). It is believed that costly nano-Fe_3O_4 used to produce the Opt 4 was responsible for the expensive product cost despite high volume FA utilization at 35%.

4.3.2. Response of LA Abrasion Test

The LA Abrasion test was completed for four different mixes cured submerged in water for 28 days, in which the Opt 5 had the most mass loss of all. It lost 59% of its initial mass after 300 revolutions, which was much higher than ~30% mass loss for others. The control specimen seemed to lose a more mass in the early stage of the test up to 300 revolutions than the Opt 1 and Opt 4. However, the Opt 1 and Opt 4 specimens lost more mass than the control specimen afterwards. Figure 9 shows the pictures of the specimens before and after the test.

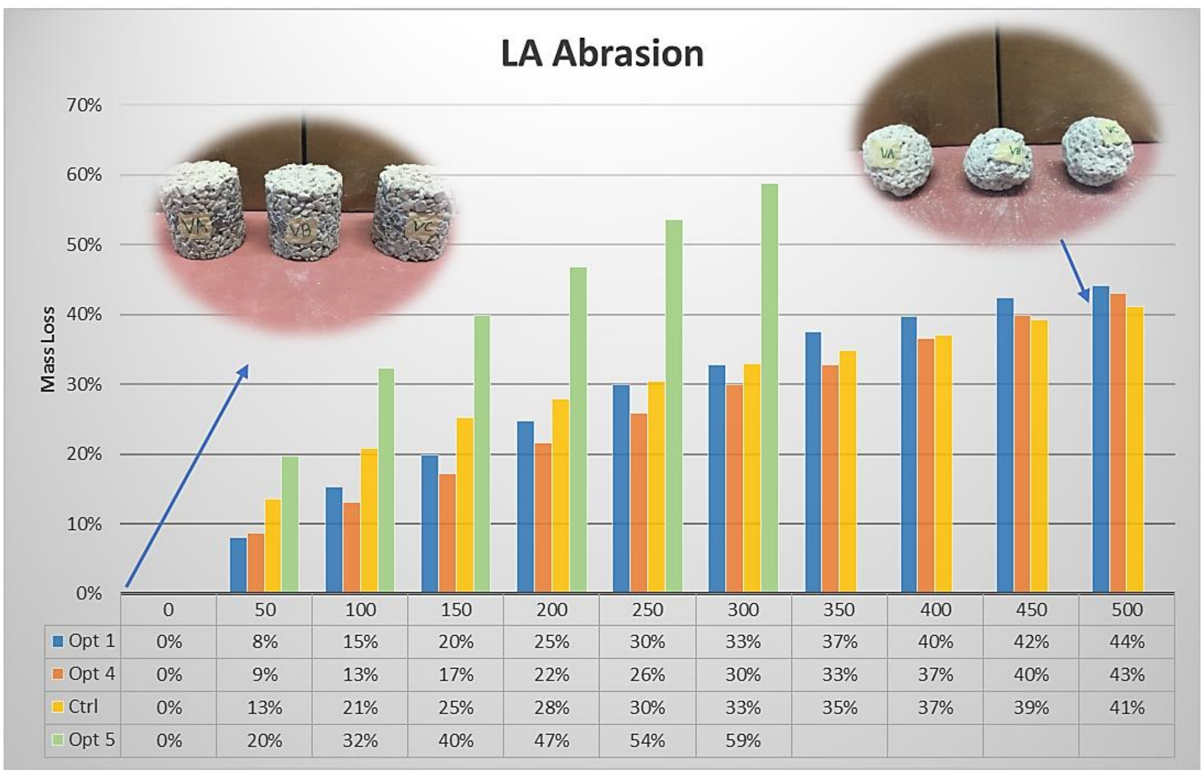

	0	50	100	150	200	250	300	350	400	450	500
Opt 1	0%	8%	15%	20%	25%	30%	33%	37%	40%	42%	44%
Opt 4	0%	9%	13%	17%	22%	26%	30%	33%	37%	40%	43%
Ctrl	0%	13%	21%	25%	28%	30%	33%	35%	37%	39%	41%
Opt 5	0%	20%	32%	40%	47%	54%	59%				

Figure 9. LA Abrasion test results

Chapter 5: Rain Simulation Chamber

Six PC mixes tested for strength, permeability, durability and costs in Chapter 4 were evaluated for their water quality performance in this chapter. The experiment was done in a rain simulation chamber with tap water spraying on the surface of the PCP as a simulation of rain precipitation and with a contaminated water applying to the PCP as NPS water.

5.1. Materials

5.1.1. Cement, Fly Ash, Nanoparticles

The same cement, FA, and nanoparticles that were described in chapter 5 were used. Therefore, they are not included in this chapter.

5.1.2. Coarse Aggregates

Coarse aggregates were used for two different purposes: the preparation of the PC and the storage of the filtered water. The limestone gravel for the PC had a diameter 4.75-12.5 mm, and the storage gravel of 12.5 mm. The gravel was purchased at a local store, and was sieved, cleaned, and dried prior to use.

5.1.3. Wooden boards, Buckets, and Pipes

The wood was used for the construction of a rain simulation chamber to simulate the rain precipitation specific to the area of El Yunque, P.R., with an intensity of a 5-year storm for a duration of 24 hours. The PCP and storage gravel was placed in the 5-gallon plastic buckets where underdrain pipes will be installed at three different elevations: top, middle, and bottom. The buckets used a water level, which was used to validate the height of water inside the system while it was running. The chamber had a drainage system made with PVC pipes and was operated for periods of 30 minutes. The wooden boards, buckets, and pipes were purchased at a local hardware store.

5.1.4. NPS Water

Treated wastewater effluent, collected at a local wastewater treatment plant prior to disinfection process, was used as an NPS water. To increase the concentration of nitrate and phosphate in the NPS water, a commercial fertilizer was spoked to the treated wastewater effluent.

5.2. Methodology

5.2.1. Chamber Preparation

The chamber was constructed of wooden boards with a dimension of 1.8 m long, 0.9 m tall and 0.2 m wide. It had four buckets for the different PCP specimens, as shown in Figure 10. Tap water was applied through the spray nozzles connected to the pipes and a pump that controlled the water pressure and therefore the flowrate (Figure 11). The NPS water was pumped on the surface of the PCP specimens at a flowrate ratio to rainwater of 1 to 10.

The system was run in four phases. Each phase was run on two times per week for two weeks as explained below:

- First phase: rainwater only
- Second phase: rainwater and NPS water.
- Third phase: neither rain nor pollutants-containing water to simulate a drought period.
- Fourth phase: rainwater and NPS water with elevated concentrations of phosphorus and nitrogen.

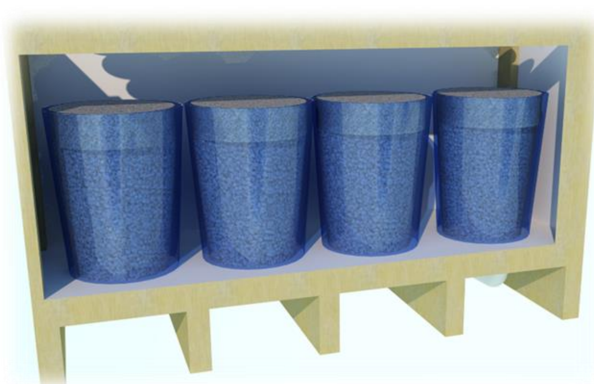

Figure 10. Rain simulation chamber sketchup

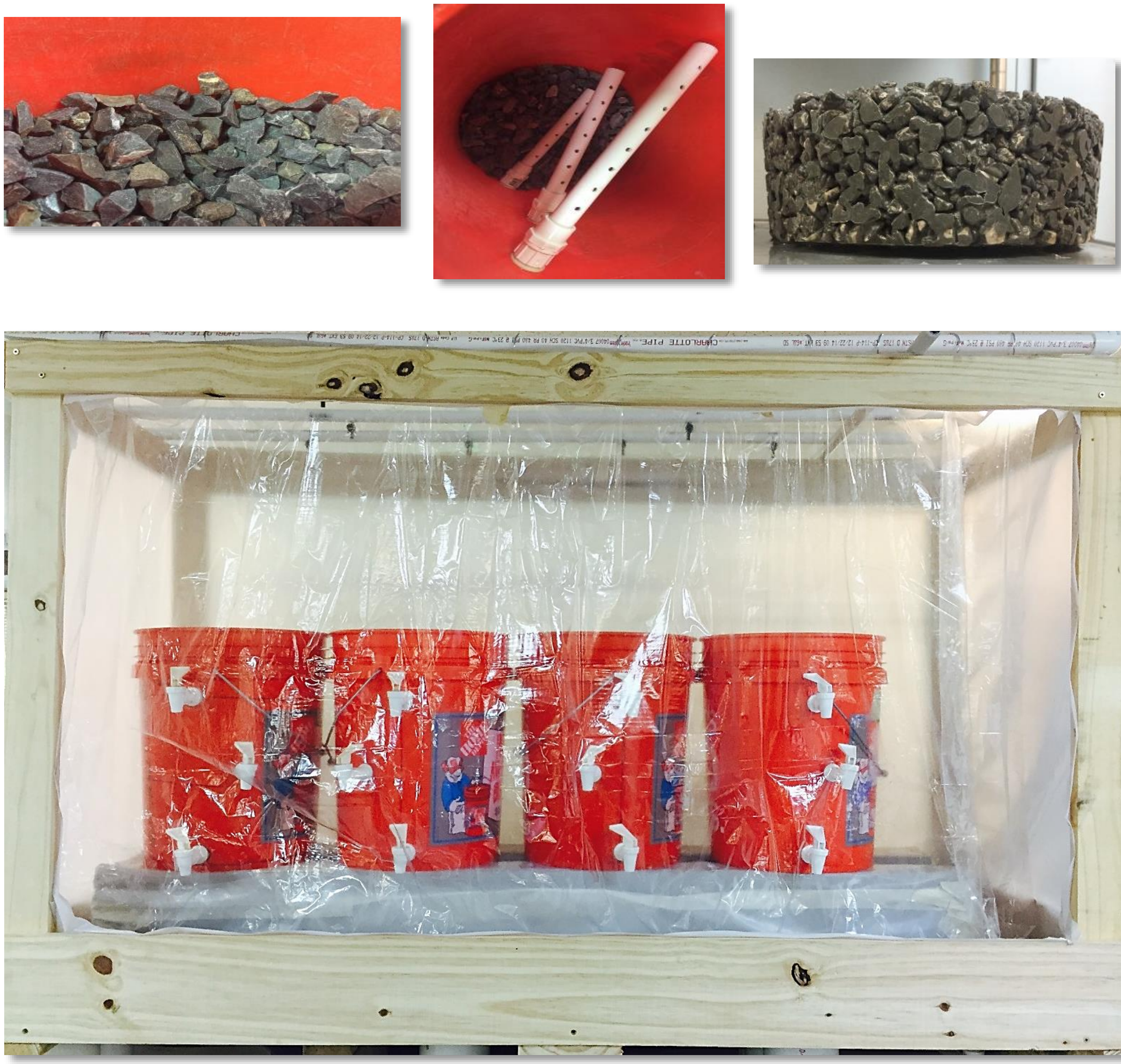

Figure 11. Rain simulation chamber construction

5.2.2. Pervious Concrete Pavement (PCP) Preparation

The Pervious Pavement Design Guidance from California (Caltrans, 2014) was used as a reference for preparation of PCP. One of the most important factors that should be carefully taken into consideration when making PCP system the depth of the reservoir and PC layer. The depth of the reservoir was calculated with the void ratio of the soil and the 85 percentile for a 24 hour rain event, in this case for El Yunque, as a means of the worst-case scenario. In order to adapt the experiment for a laboratory scale, the PCP was scaled down by 50%. The reservoir and PC depth was 25.4 cm and 10.2 cm, respectively. The reservoir had a gravel in size of 12.5 mm and the PC of 4.75 to 12.5 mm. A total of six circular PC were made as shown in Table 10 and Figure 12. It should be noted that Table 10 shows the ratios of five optimum mixes and one control and that the type GU cement which was used for the Opt 1, Opt 2, Opt 3 and control, while the type IP cement was used for Opt 4 and Opt 5.

Table 10. PCP compositions in percentages of different factors

FACTORS	**PCP**			
	Opt 1	**Opt 2**	**Opt 3**	**Ctrl**
Fly Ash (FA/B)	24	26	0	0
Nano-Silicate (NS/FA)	1.9	0	1	0
Liquid (W/B)	32	32	32	33
Water Reducer (SP/B)	0.35	0.25	0.20	0

FACTORS	**PCP**	**FACTORS**	**PCP**
	Opt 4		**Opt 5**
Fly Ash (FA/B)	35	Fly Ash (FA/B)	60
Nano-Iron (NI/B)	6	Nano-Silicate (NS/B)	0.04
Liquid (W/B)	36	NaOH (mole/L)	50
Water Reducer (SP/B)	1.2	Liquid (NaOH/B)	40

Figure 12. PCP specimens (25.4 cm in dia. x 10.2 cm in thickness)

5.2.3. Water Quality Analysis

Rainwater, NPS water and effluent from the PCP systems were tested for water quality analysis. The water infiltrated through the PCPs was sampled from the top sampling post while the system was running. After 8 hours, gravel storage water was sampled from the bottom sampling post. The stored water in the gravel layer was drained and the systems were put in a standby made until the next rain simulator.

The water quality parameters analyzed were pH, conductivity, turbidity, phosphorus, nitrogen, total organic carbon (TOC), and FC. A 0.45-μm cellulose ester membrane was used as a membrane filtration technique for FC analysis. The membranes were put in a petri dishes that will contain HACH m-FC broth. They were incubated for 24 hours at 44.5°C, and blue colonies were considered as FC colonies. Table 11 shows the instruments that were used for each water quality parameter to be measured.

Table 11. Instruments used for water quality quality analysis

Parameters	Instrument that will be used
pH	Oakton pH meter
Conductivity	PCSTestr 35 Multi-Parameter
Turbidity	2100P Turbidimeter
Nitrate and Phosphate	UFLC Shimadzu ion chromatograph
TOC	Teledyne Tekmar

5.3. Results and Discussion

5.3.1. Water Quality

Changes of physical, chemical and biological characteristics of water quality due to a new infrastructure implementation need to be assessed to ensure quality of the environment. As such, the pavements that are going to be implemented are to be assessed to know the impact on the water quality. The impervious pavement transports contaminants to water sources, whereas the PC captures the contaminated water and filters the water as it passes through the matrix. Six different mixes were tested with the rainfall simulation with NPS pollutants. The water quality parameters measured were pH, turbidity, nitrate, phosphate, TOC and FC. Figures 13 - 17 show the results obtained from the analysis of the influent and effluent water of the six different mixes. All the graphs have the specimens called Opt and the notation "B" indicates the results of the storage gravel. In addition, every graphs contain the phases explained in the Methodology section. The detailed results are provided in the Table 1-4 in the Appendix.

Figure 13 show that pH was slightly lowering as the experiment proceeded. Generally, the Opt 1, Opt 2, Opt 3 and Ctrl had a range from 7 to 9, whereas the Opt 4 and Opt 5 had a pH range from 8.4 to 12. The Opt 5 had the highest pH because it was a geopolymer PC that was made of the greatest amounts of FA of all and, it was alkali-activated with NaOH. Turbidity was decreasing phase by phase (Figure 14). The nitrate concentrations in the effluents demonstrate the similar levels to those in the influent with some fluctuations (Figures 15). For TOC, the Opt 4 and Opt 5 were superior to others (Figures 16).

The PC also reduce FC as shown in Figure 17; one can observe that the ones that had less pH removed more FC than the effluent with the highest pH. According to literature, FC has a higher survival rate in stormwater with a pH at ~7 as opposed to stormwater with higher pH levels (Neger, 2002). However, in the phase 4 that had an added amount of fertilizer, all the optimums reduced FC more than 80% of the FC, regardless of the levels of pH.

It is believed that dissimilar physiochemical and biological mechanisms were responsible for the removal of different pollutants in this study. For examples, FC removal could be attributed to alkaline properties of PC matrix and resulting water. In the case when pH in infiltrating water was not in alkaline range, then adsorption to PC and/or gravel surfaces would be responsible for FC removal. Precipitation and/or adsorption could be responsible for the P removal. Therefore, further investigation is warranted to elucidate the mechanisms of pollutant-specific removals through PC systems.

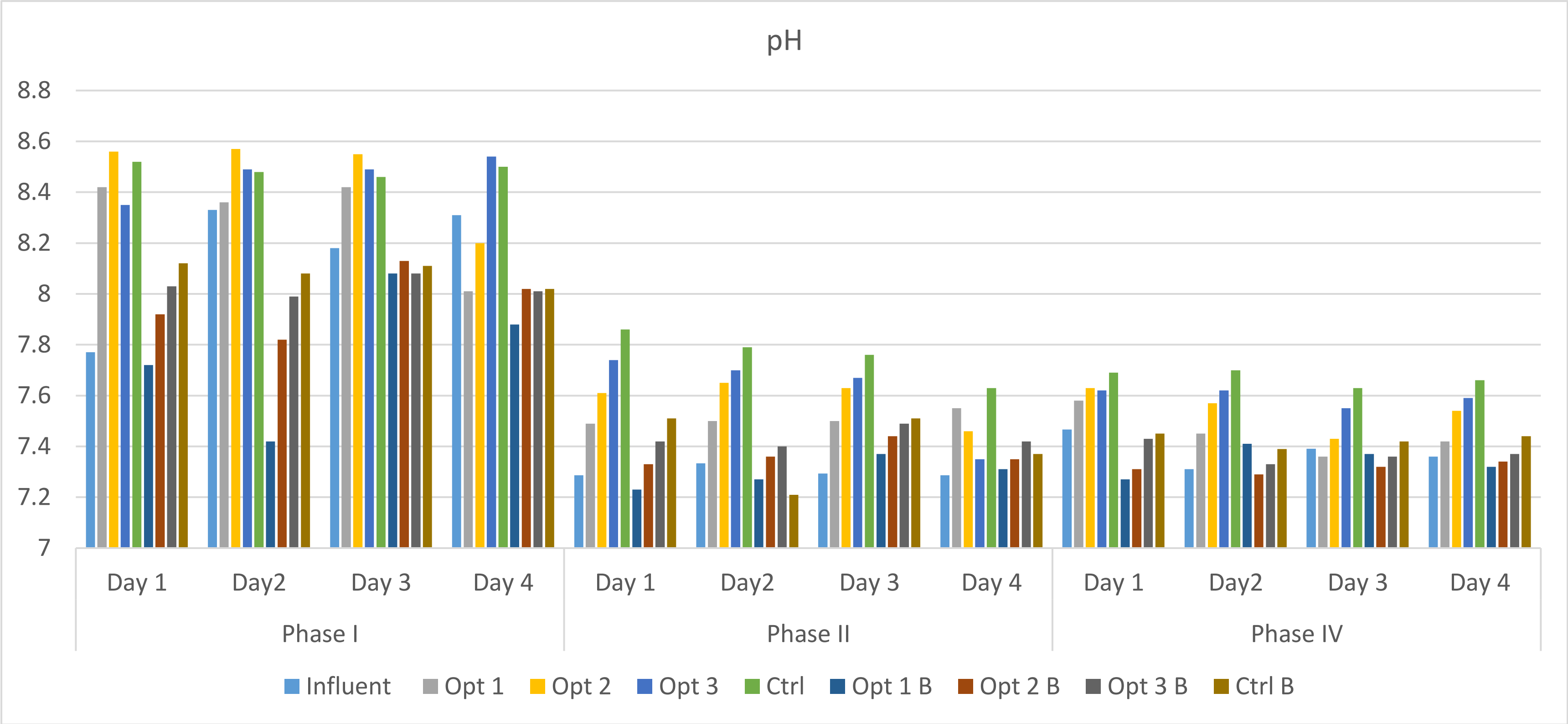

Figure 13. Results of pH in three different phases

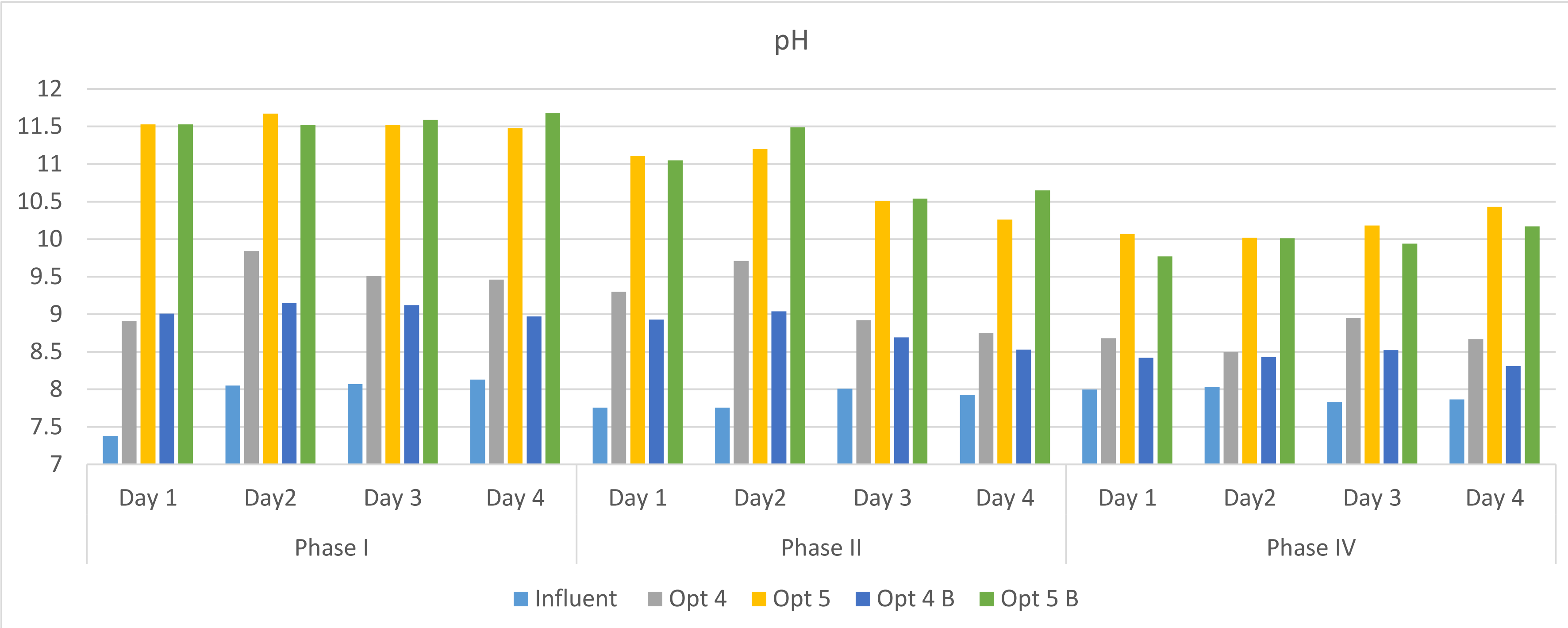

Figure 13. (Continued).

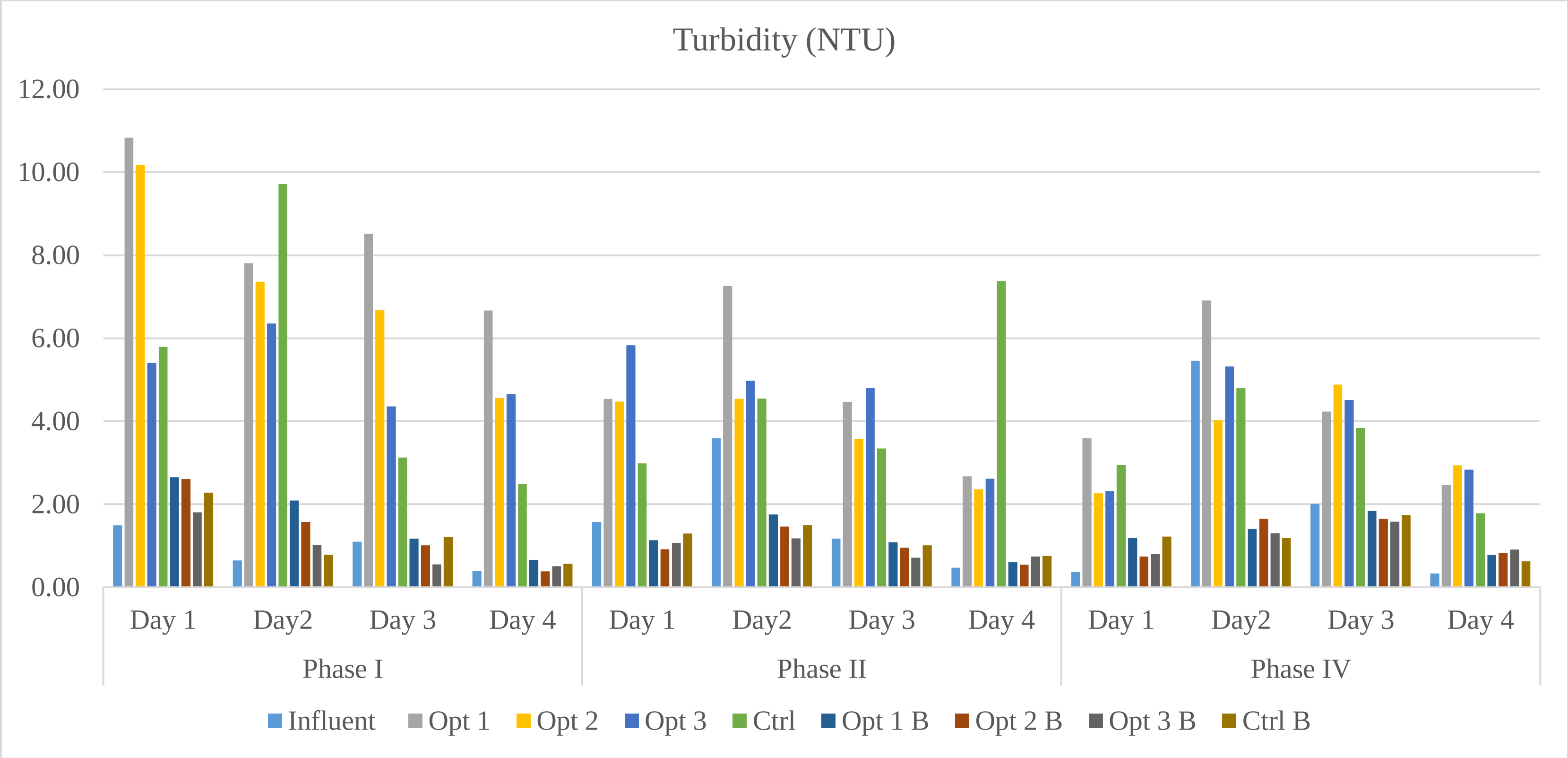

Figure 14. Results of turbidity in three different phases

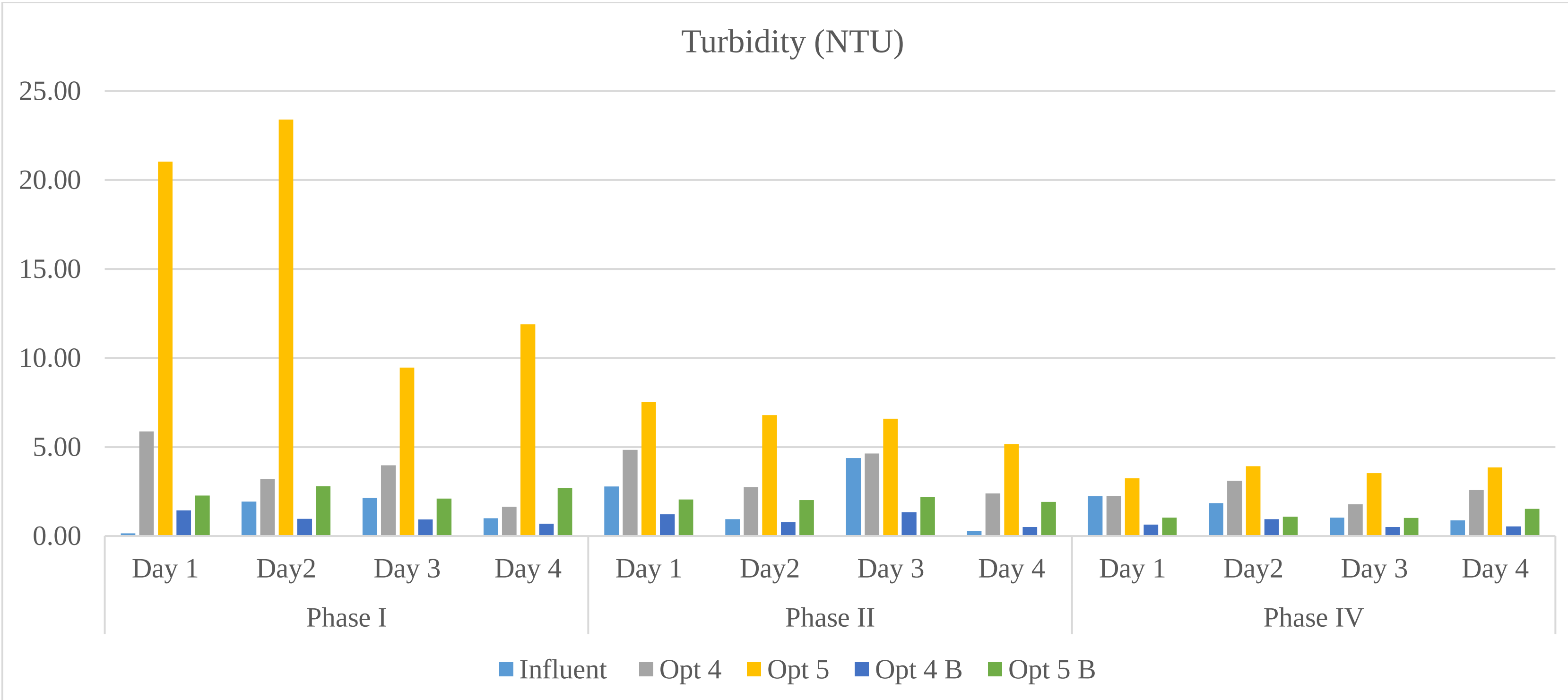

Figure 14. (Continued).

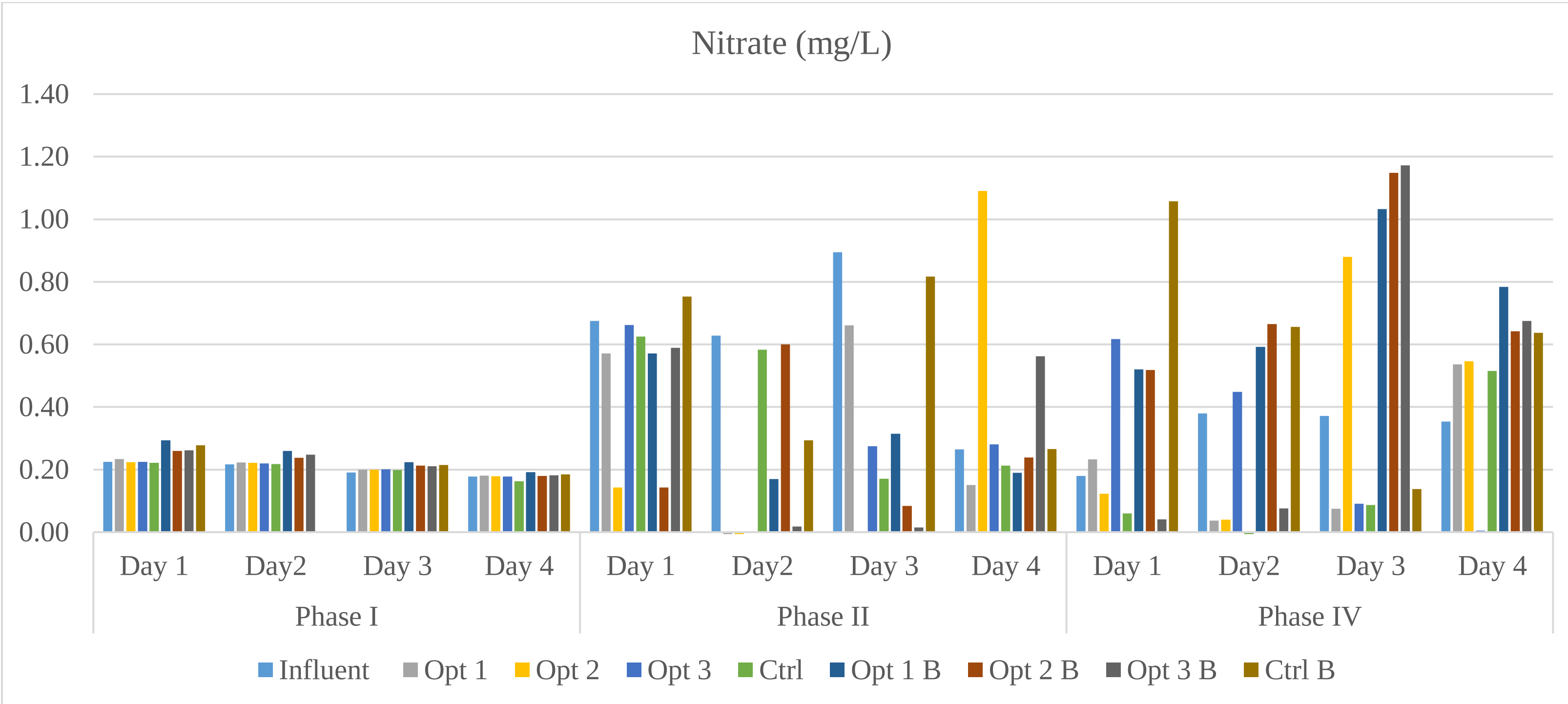

Figure 15. Results of nitrate in three different phases

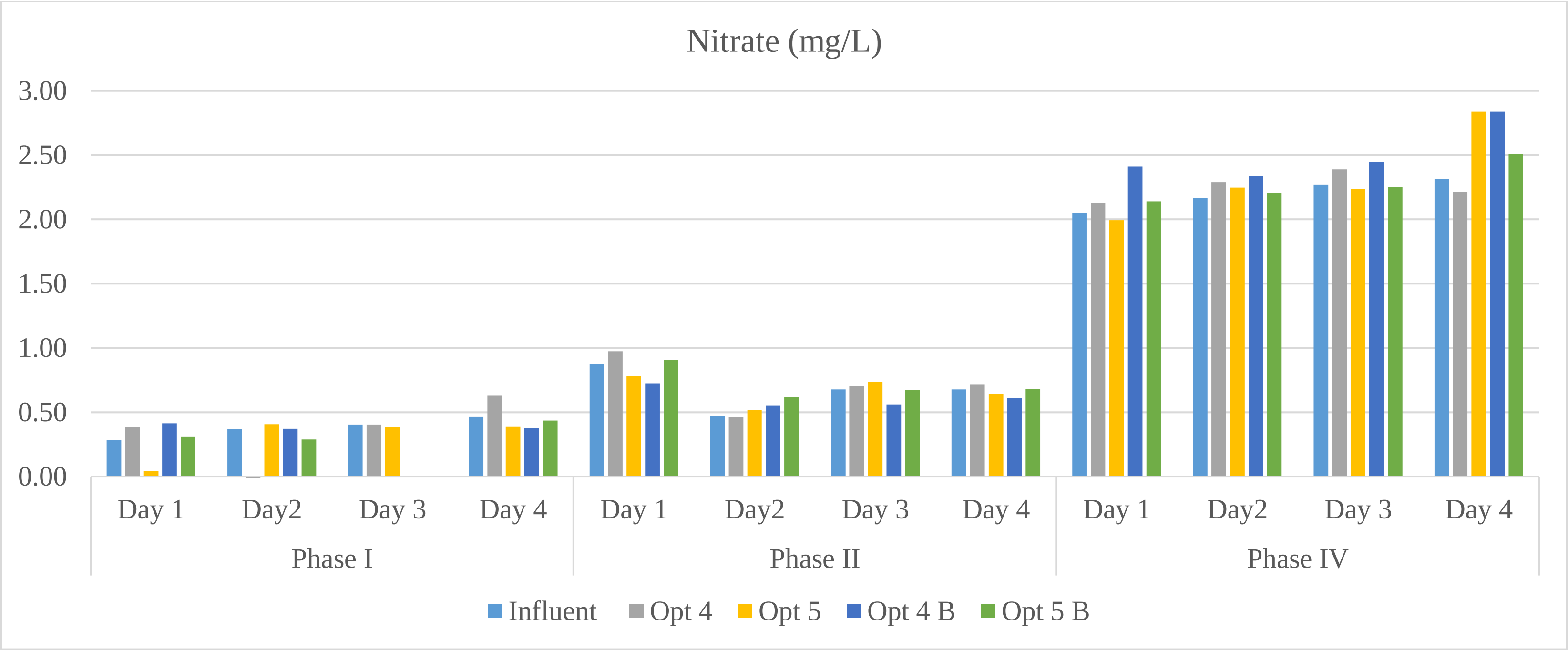

Figure 15. (Continued).

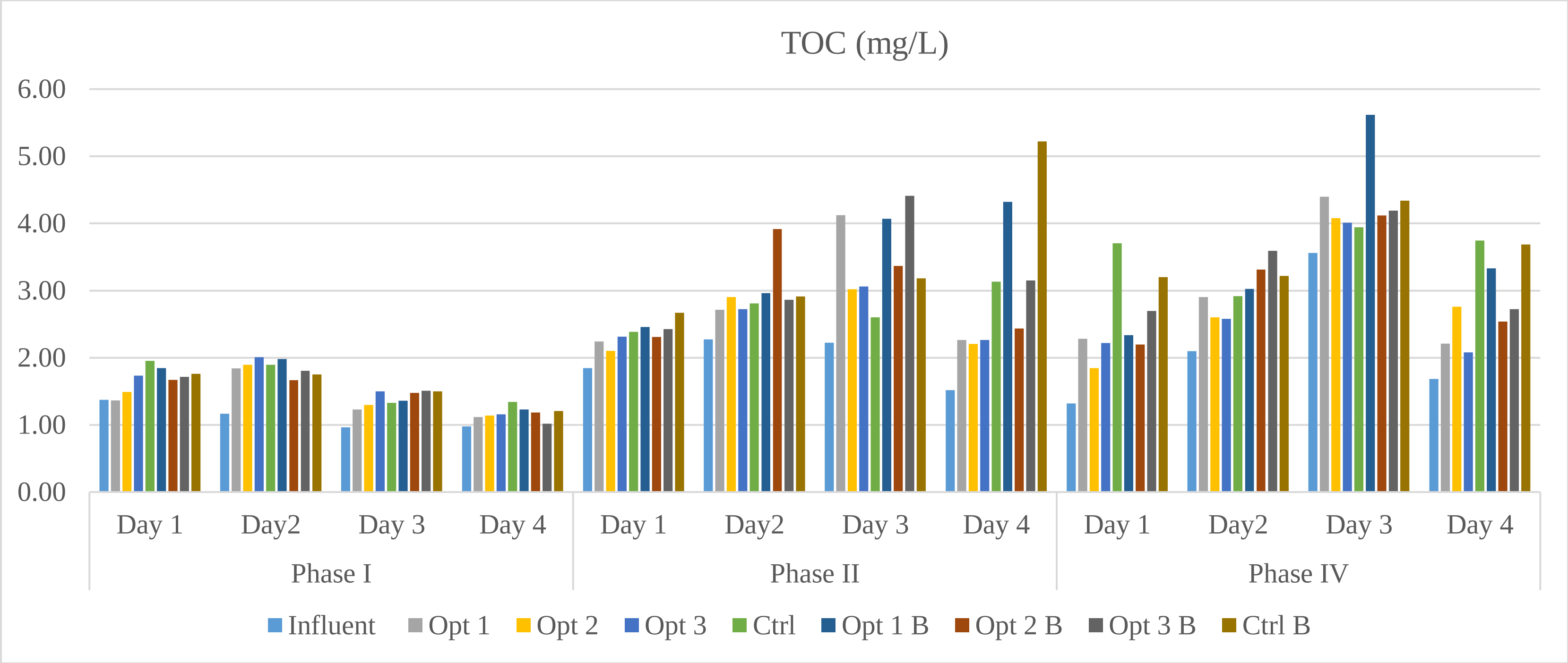

Figure 16. Results of TOC in three different phases

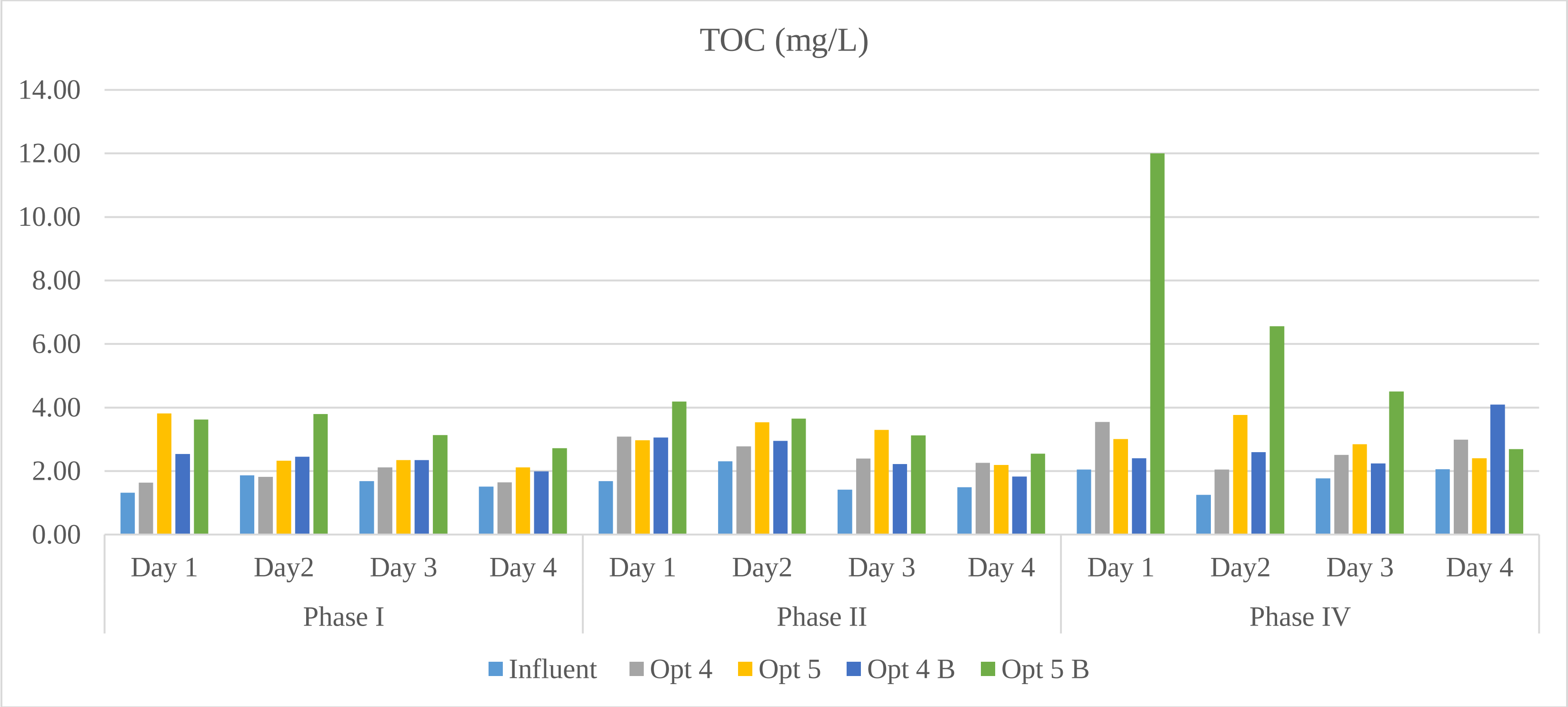

Figure 16. (Continued).

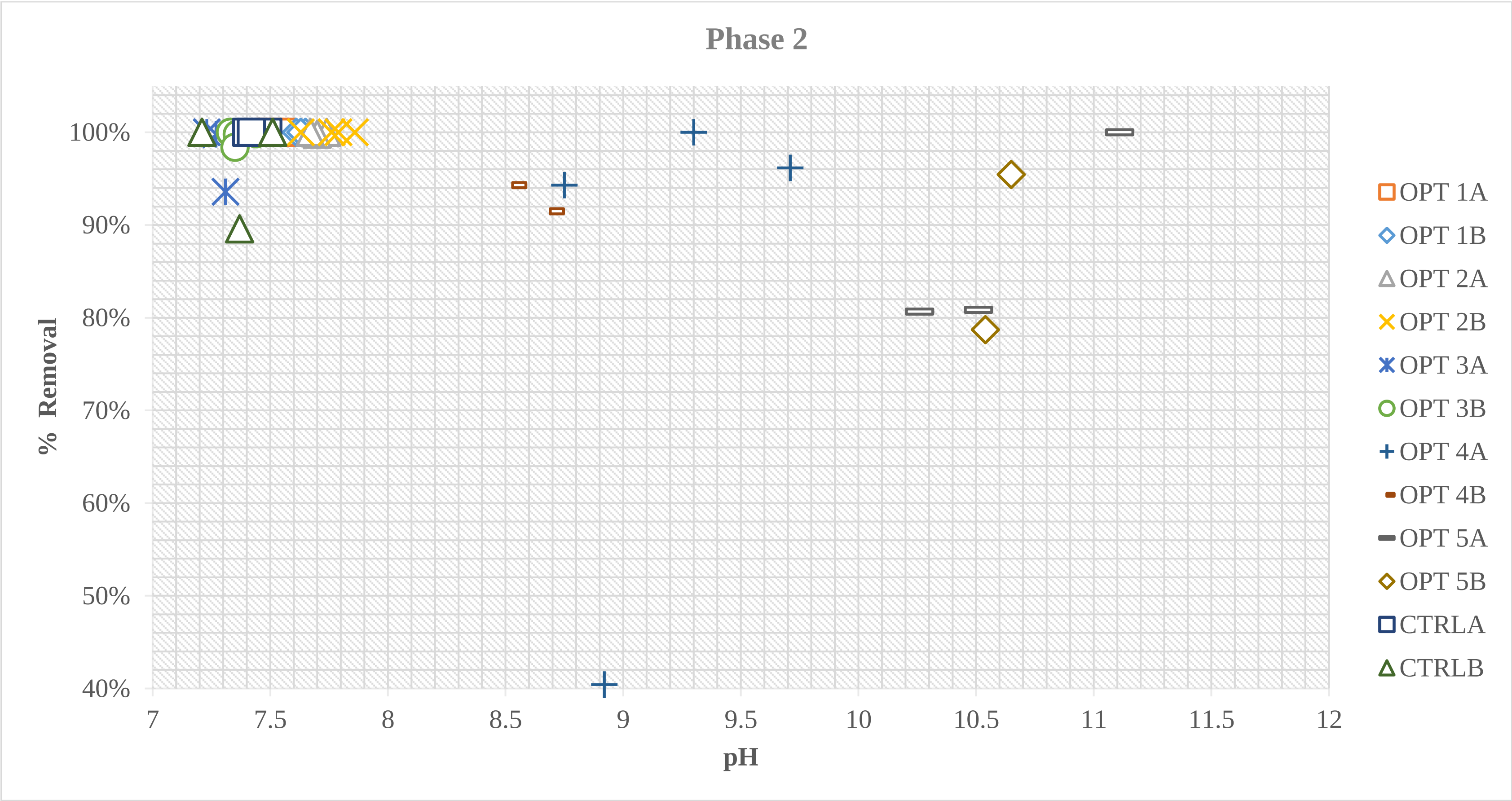

Figure 17. FC percentage removal versus pH

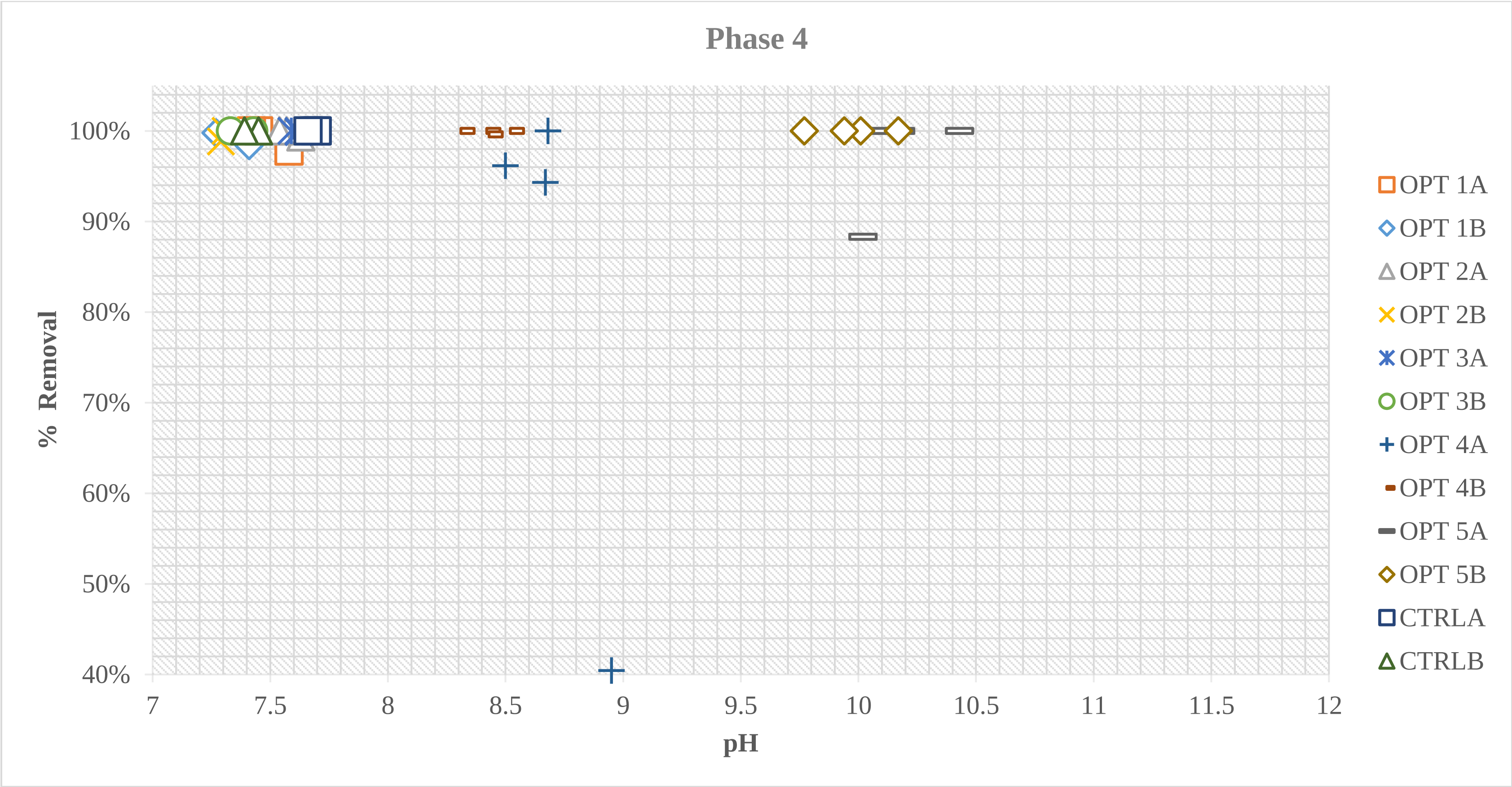

Figure 17. (Continued).

Chapter 6: Water Quality Validation of PCPs

The results of FC removals in relation to the pH strength found in the previous chapter were unusual. That is, a better FC removal was achieved at a lower (~normal) pH levels. Therefore, it was necessary to evaluate again to ensure of the influence of pH on the FC removal. To this end, the systems scaled down by 10% were constructed. The same materials described in the previous chapter were used.

6.1. Methodology

6.1.1. Scaled-down PCP Systems with Rain Simulation

For a better rain simulation, each system was designated with its own rain spray nozzle from which the same strength of rain was applied to the systems. Also, the systems were made in duplicate. It is important to know that, in this experiment, four mixes were tested not six mixes. They were the Opt 1, Ctrl, Opt 4 and Opt 5. Figure 18 show the setup of the scaled-down experiment.

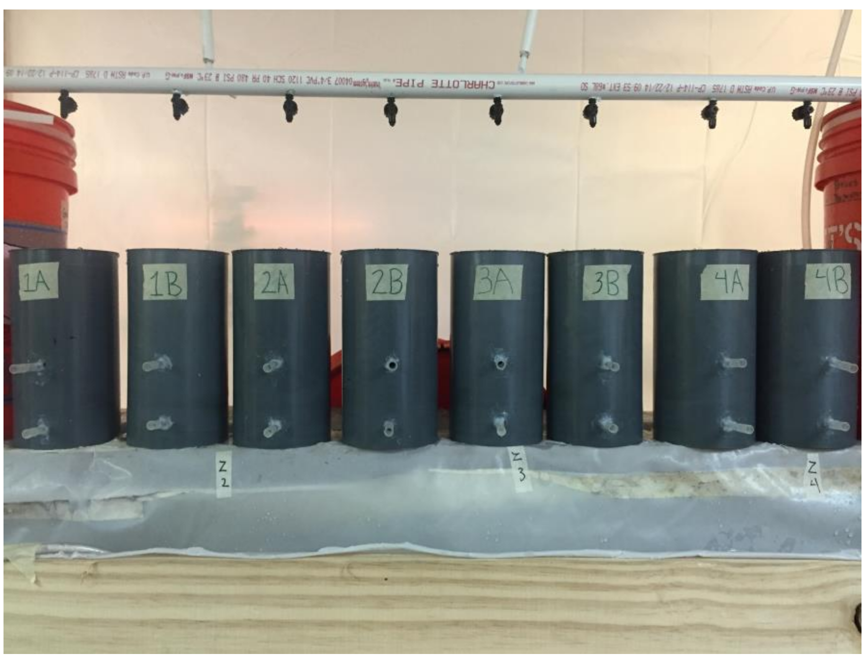

Figure 18. Scaled-down systems in the rain simulation chamber

6.2. Results and Discussion

6.2.1. Water Quality

The pH values found in the current experiment (Figure 19) were similar to those from the previous experiment shown in Figures 13. However, an exception was observed for the Opt 4 where the pH appeared lower. In general, the nitrate concentration was not reduced by the PCP systems (Figure 21). Unlike to the phosphorus removal at 100 % shown in previous chapter (Figure 14), all the systems tested in this chapter had an increased phosphorus concentration (Figure 22).

Again was found a better FC removal at lower (~neutral) pH ranges than a higher alkaline pH ranges (Figures 23). This unique finding needs to be further investigated to understand scientific reasons for the underlying mechanisms responsible for a better FC removal at neutral pHs.

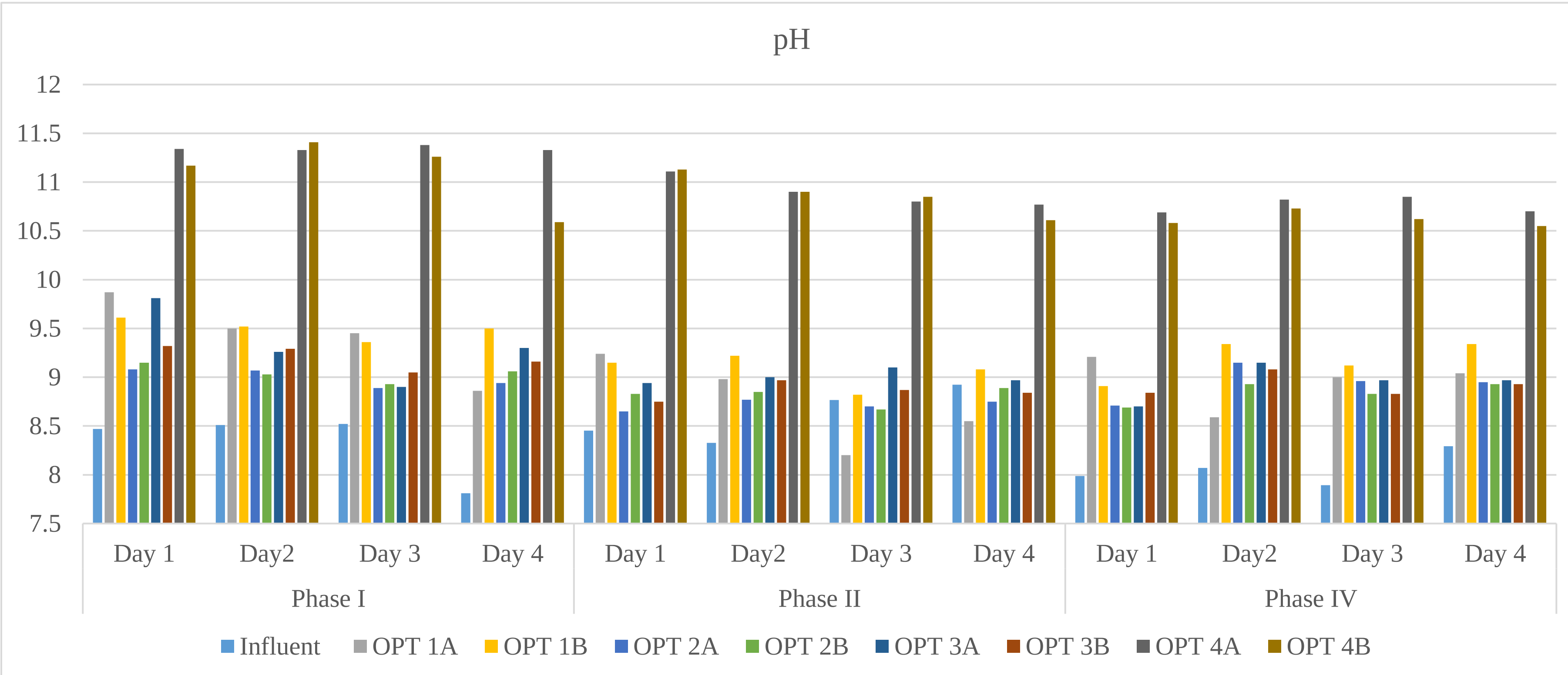

Figure 19. Validation results of pH

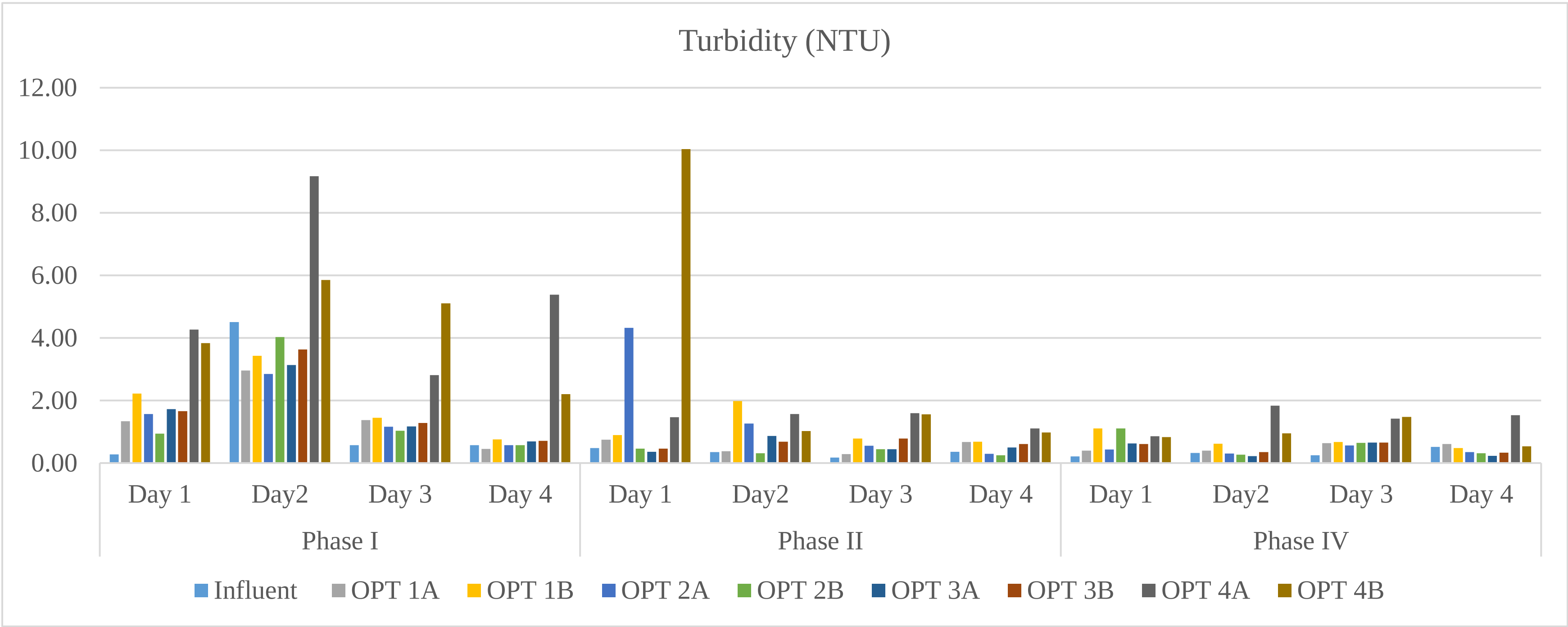

Figure 20. Validation results of turbidity

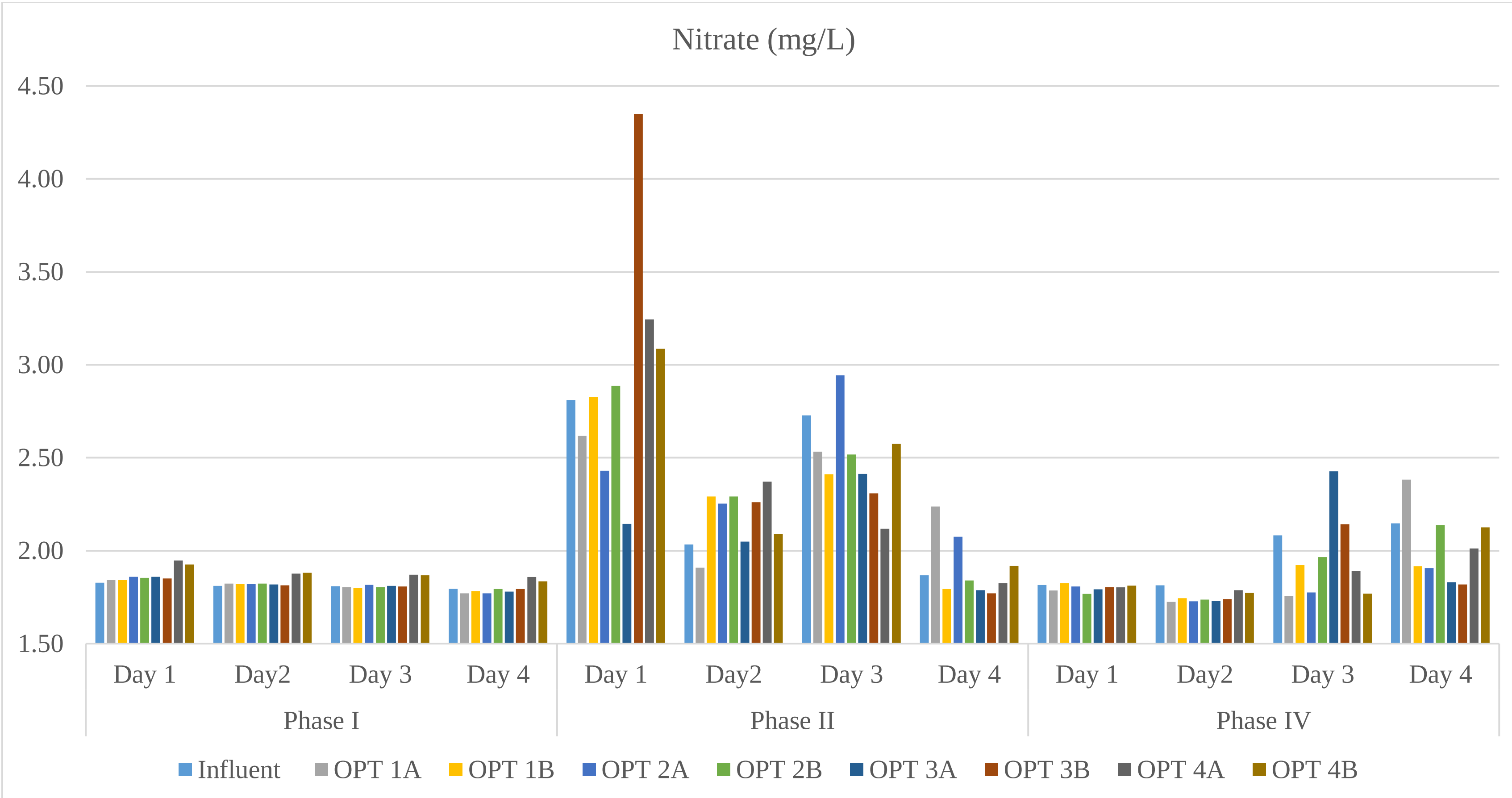

Figure 21. Validation results of nitrate

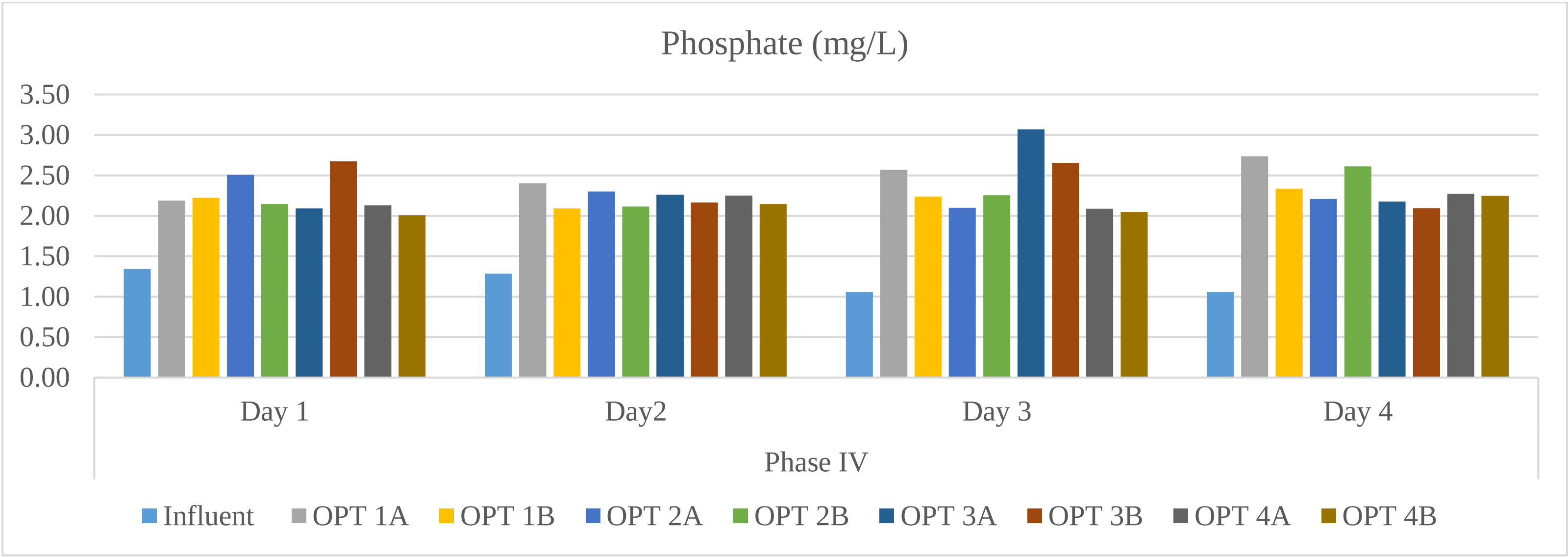

Figure 22. Validation results of phosphate

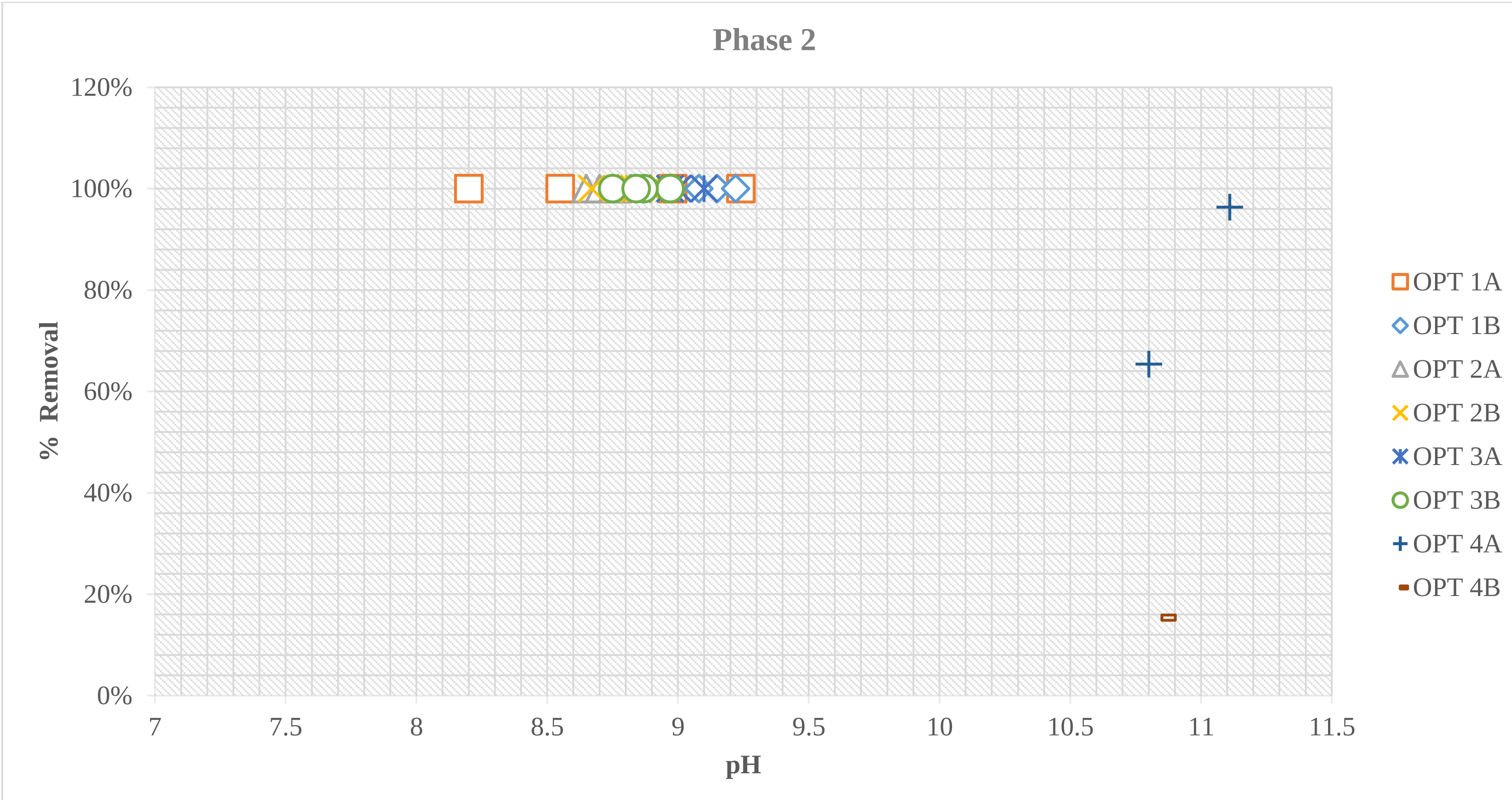

Figure 23. Validation of FC percentage removal versus pH

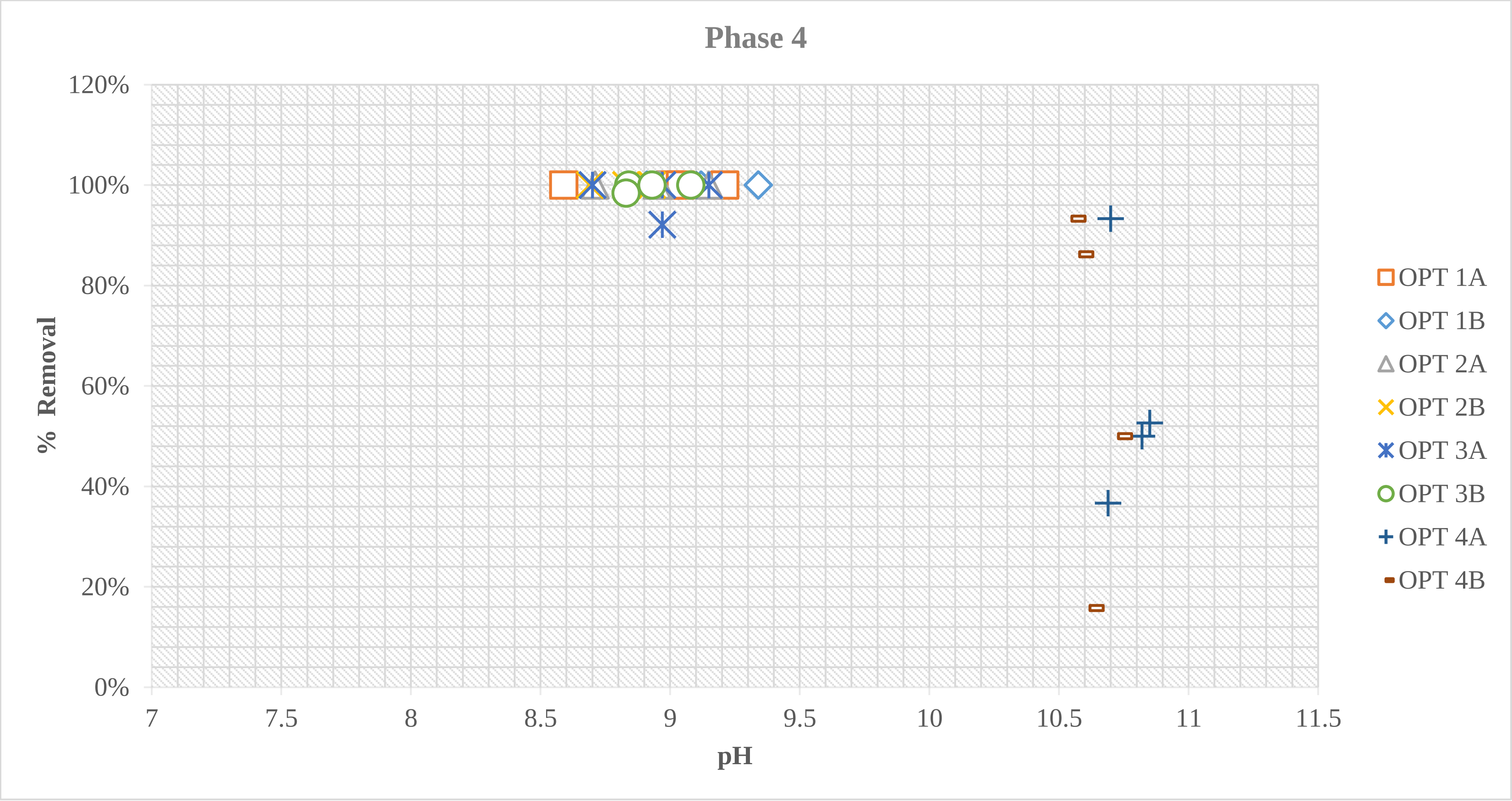

Figure 23. (Continued).

Chapter 7: Implementation of Optimum PCP

In this chapter, the design and construction of a field PC site where the Opt 1 was implemented is included. The site had frequent ponding with rainwater accumulated on the impervious surfaces. The Opt 1 was chosen based on the properties, costs and water quality performance as described in the previous chapters.

7.1. Methodology

7.1.1. Design of PCP

The site has a water storage depth of 4-5 inches with 2-in gravels. Below the storage layer a geotextile was placed to keep the soil from intruding the storage layer. The storage depth was determined based on the precipitation, depth of 1.04 inches for 15 mins with 2-year storm event in Mayaguez, P.R. (Atlas, 14). A perforated 3-in underdrain pipe was embedded to discharge collected stormwater to the stormdrain nearby the site. A 3-in vertical monitoring well was installed to observe the depth of the stored stormwater and to do water quality monitoring in the future. Between the PCP slab and the gravel storage layer a screen mesh was placed as a choker.

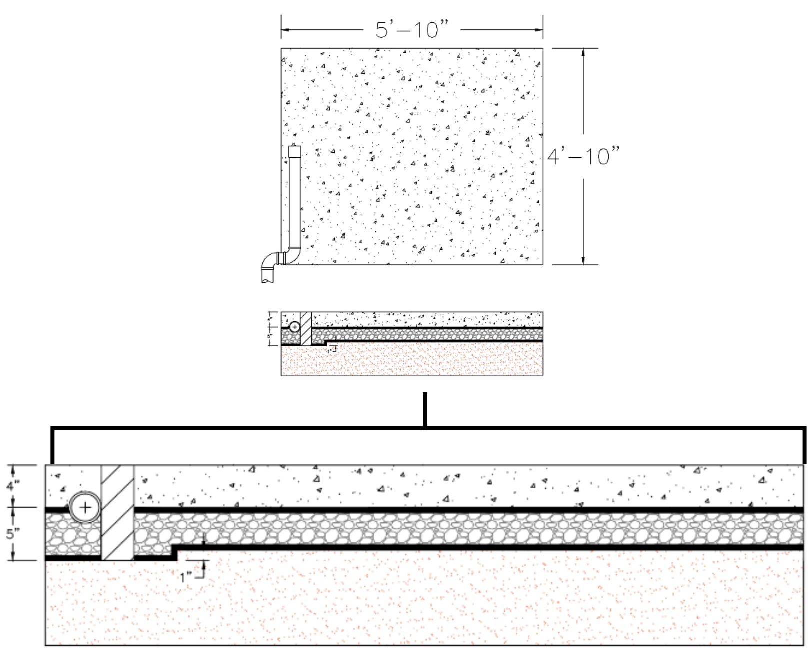

Figure 24. Design of PCP for the field implementation

7.1.2. Implementation of the PCP at Field

The existing impervious concrete slab was demolished and the site was excavated to the depth as depicted in Figure 25. After leveling and grading of the site (Figure 25a), the geotextile was laid on the top of the subgrade soil (Figure 25b) and 2-in water storage gravel was placed (Figure 25c). As a choker layer, a screen mesh was placed on the top of the storage gravel layer (Figure 25d). The PC was mixed in a 12-ft^3 mixer (Figure 25e) and placed at the site (Figure 25f). The site was cured covered by a plastic for 14 days and was opened for public use (Figure 25g). The surrounding area will be re-developed with more environmentally friendly setting where PCP will also be placed in part of the area (Figure 26).

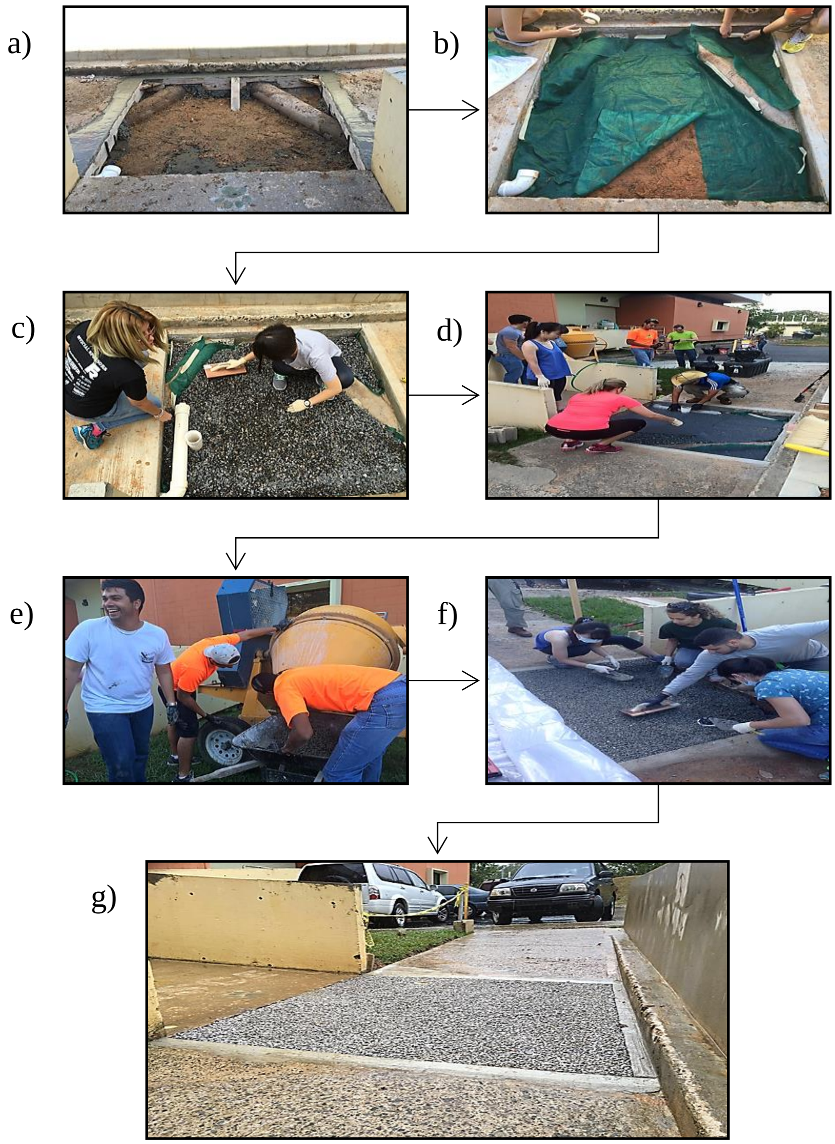

Figure 25. Construction procedures of the field PCP implementation

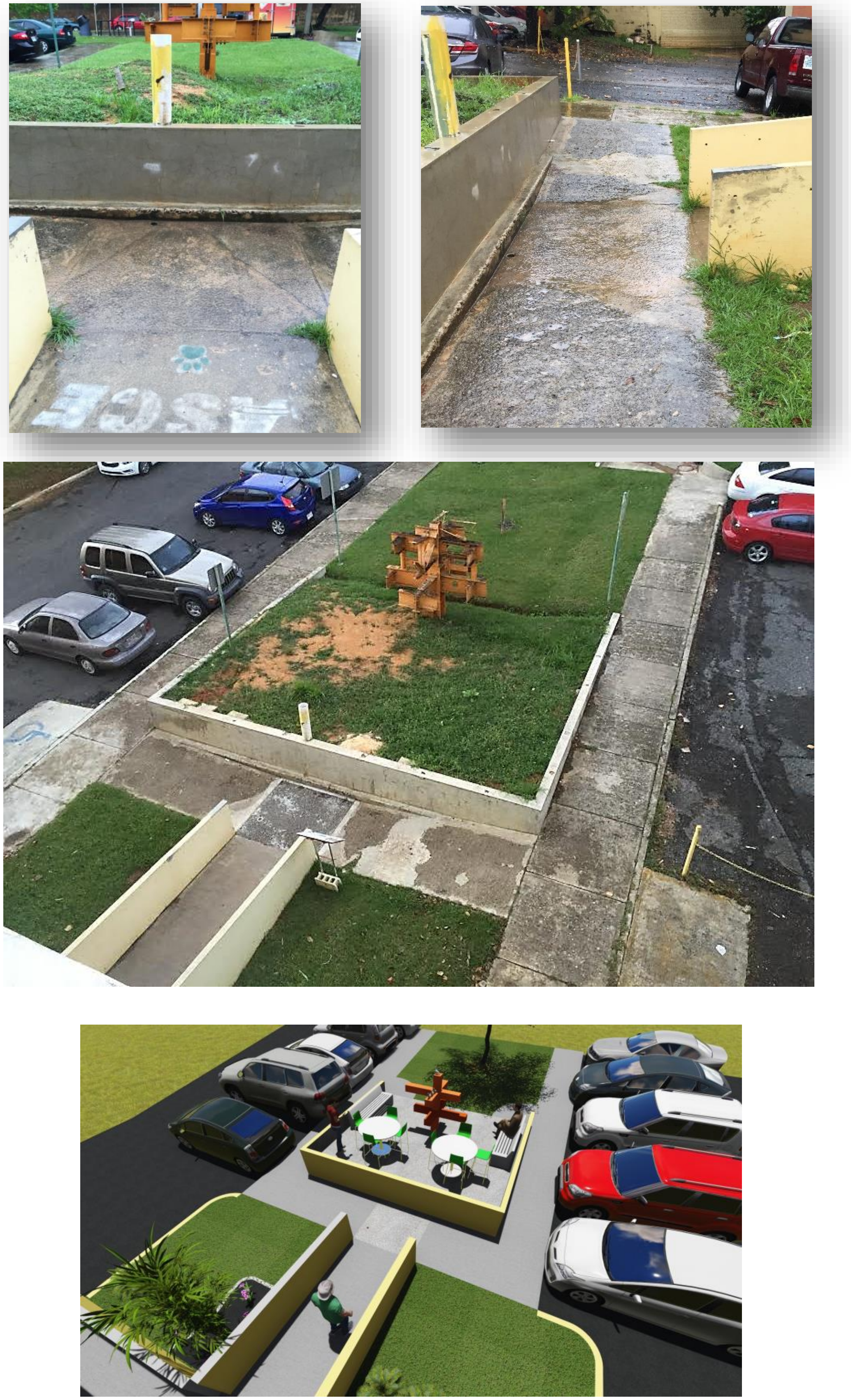

Figure 26. Site view before and after the PCP implementation at the field

The use of appropriate tools turned out to be critical for the success of the site construction. Only tools used for compaction were manual tampers and hand trowels during the construction. A compaction roller should have used for more even placement of PC at the site.

It is always recommended to make more pervious concrete than the calculated quantity. In fact, a more pervious concrete by ~15% was needed for the site completion. It should be noted, however, that the extra quantity of pervious concrete needed would depend on the mix design, especially on the gravel size, and the extent of compaction.

7.1.3. On-going Monitoring and Maintenance

The site was open available for public use in January 30, 2016. On-going routine monitoring of the site has been provided for checking surface raveling, debris deposition, and clogging. No noticeable surface raveling was found on the surface but surface clogging due to debris deposition has been an issue that had a negative effect on the field PCP performance. Debris deposition was mostly due to the leftover grass clippings accumulated on the PCP surface and the sandy debris transported with run-on water from the ramps.

As such, the following routine and regular maintenance activities have been given to the site:

- Routine maintenance: debris blowing and vacuuming on the PCP surface, especially right after grass cutting.
- Regular maintenance: cleaning the PCP surface with a pressure water jet and vacuum, simultaneously.

It is important to mention that, although not included in this current project, the research group has a future plan to make water quality performance at the site. Also, site-specific monitoring and maintenance guidelines will be developed and handed in to the university administration in order to ensure an appropriate performance of the site.

Conclusions

The following conclusions can be made based on the lab-scale experiment and the field implementation of PCP:

- The RSM made of 30 different specimens, the optimum PCP had 32% L/B, 24% FA/B, 1.9% NS/FA and 0.35% SP/B, with a predicted maximum 28-day compressive strength and permeability at 17 MPa, and 8.1 mm/s, respectively.
- The greatest 28-day compressive strength was found for the Opt 1 (17.2 MPa), followed by the Opt 4 (16.2 MPa), Opt 2 (14.4 MPa), Opt 3 (10.5 MPa), control (9.6 MPa) and Opt 4 (4.7 MPa). Permeability of the six mix specimens were higher than 5.0 mm/s, with the Ctrl and Opt 5 having the greatest (15.0 mm/s) and the lowest (5.0 mm/s), respectively. The production costs of the Opt 1, Opt 2, Opt 3, and Ctrl were approximately $280/yd^3. The Opt 4 had the most expensive production cost at ~$3000/yd^3, and the Opt 5 at ~$500/yd^3. Figure 27 shows a synopsis of the compared compressive strength, permeability and the costs.

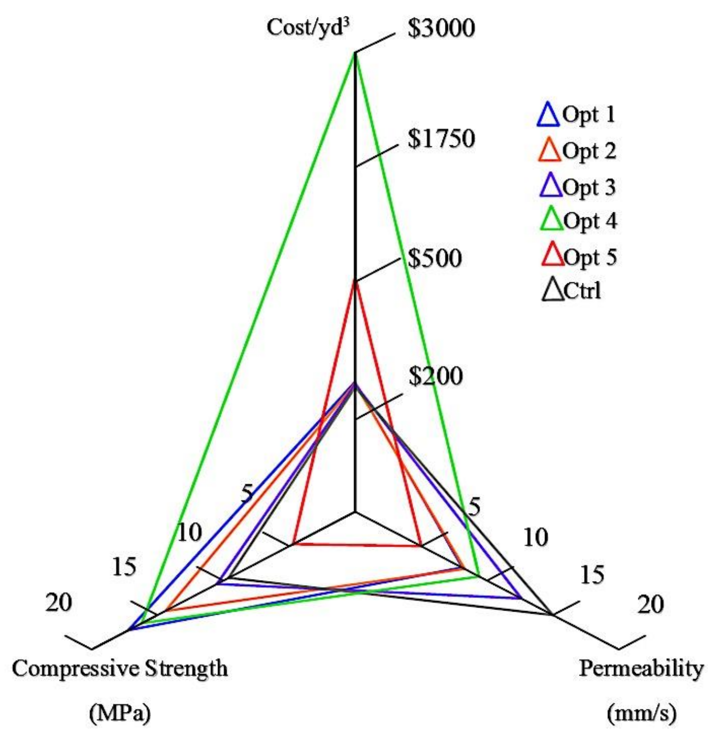

Figure 27. 3D plot of PC comparison with the responses

- Among the six PCP systems tested, a better water quality performance was observed for the Opt 1, Opt 2, Opt 3, Opt 4 and Ctrl than the Opt 5. All the PCP systems were capable of removing FC at 100% even at neutral pHs.
- The Opt 1 was chosen for the field implementation based on its quality of the strength, permeability and costs. The field site was constructed and is in use now. In fact, it was the first field implementation of nanotechnology-enabled pervious concrete pavement in Puerto Rico.

Bibliography

Abdel-Raouf, N., Al-Homaidan, A.A., Ibraheem, I.B.M. (2012). Microalgae and wastewater treatment. Saudi Journal of Biological Sciences Vol 19, 257-275.

Abegunrin, T.P., Awe, G.O., Idowu, D.O., Adejumobi, M.A. (2016). Impact of wastewater irrigation on soil physico-chemical properties, growth and water use pattern of two indigenous vegetables in southwest Nigeria. Catena Vol 139, 167-178.

ACI. (2010). American Concrete Institute. Report on pervious concrete. 1st Ed., ACI 522R-10. American Concrete Institude, Michigan.

Antoni, Chandra, L., Hardjito, D. (2015). The impact of using fly ash, silica fume and calcium carbonate on the workability and compressive strength of mortar. Procedia Engineering Vol 125, 773-779.

Asadollahfardi, G., Delnavaz, M., Rashnoiee, V., Ghonabadi, N. (2016). Use of treated domestic wastewater before chlorination to produce and cure concrete. Construction and Building Materials Vol 105, 253-261.

Amin, M., Abu el-hassan, K. (2015). Effect of using different types of nano materials on mechanical properties of high strength concrete. Construction and Building Materials Vol 80, 116-124.

Caltrans. (2014). Pervious Pavement Design Guidance. Retrieved May, 2015 from http://www.dot.ca.gov/hq/oppd/stormwtr/bmp/DG-Pervious-Pvm_082114.pdf

EPA. (2012). US Environmental Protection Agency. Stormwater runoff & impervious surfaces. Retrieved July, 2015 from http://www3.epa.gov/caddis/ssr_urb_is1.html.

EPA. (2015). US Environmental Protection Agency. Pervious concrete pavement. Retrieved January, 2016 from http://water.epa.gov/polwaste/npdes/swbmp/Pervious-Concrete-Pavement.cfm.

EPA. (2015). US Environmental Protection Agency. 2014 Greenhouse emission for large facilities. Retrieved February, 2016 from http://ghgdata.epa.gov/ghgp/main.do.

EPA. (2016). US Environmental Protection Agency. Polluted runoff: nonpoint source pollution. Retrieved February, 2016 from http://www.epa.gov/polluted-runoff-nonpoint-source-pollution/what-nonpoint-source.

Gaedicke, C., Marines, A., Miankodila, F. (2014). Assesing the abrasion resistance of cores in virgin and recycled aggregate pervious concrete. Construction and Building Materials Vol 68, 701-708.

Gagg, C.R. (2014). Cement and concrete as an engineering material: An historic appraisal and case study analysis. Engineering Failure Analysis Vol 40, 114-140.

Hill, R. (2016). Stormwater management. Retrieved January, 2016 from http://richmondhill.ca/subpage.asp?pageid=epw_stormwater_management.

Irdemez, S., Demircioglu, N., Yildizm, S.Y. (2006). The effects of pH on phosphate removal from wastewater by electreocoagulation wih iron plate electrodes. Journal of Hazardous Materials Vol 137, 1231-1235.

Jamal, H. (2014). Engineering Materials. Retrieved December, 2015 from http://www.aboutcivil.org/concrete-technology-admixtures.html.

Jo, B.W., Chakraborty, S., Kim, K.H. (2014). Investigation on the effectiveness of chemically synthesized nanocement in controlling the physical and mechanical performances of concrete. Construction and Building Materials Vol 70, 1-8.

Kelly, W.M. (2011). Mineral Industry of the State of New York. Retrieved December, 2015 from http://www.nysm.nysed.gov/publications/record/vol_03/chapter05/.

Khuri, A.I., Mukhopadhyay, S. (2010). Response surface methodology. WIREs Computational Statistics.

Luck, J.D., Workman, S.R., Coyne, M.S., Higgins, S.F. (2009). Consequences of manure filtration through pervious concrete during simulated rainfall events. Biosystems Engineering Vol 102, 417-423.

McMillan, T. (2007). Comparing traditional concrete to permeable concrete for a community college pavement application.

Mindess, S.J., Young, F., Darwin, D. (2003). Concrete. New Jersey: Pearson Education, Inc.

Minitab. (2015). What is a central composite design?. Retrieved January, 2016 from http://support.minitab.com/en-us/minitab/17/topic-library/modeling-statistics/doe/response-surface-designs/what-is-a-central-composite-design/.

Mohamed, A.M. (2015). Influence of nano materials on flexural behavior and compressive strength of concrete. Housing and Building National Research Center Vol 10, 1-14.

Montgomery, D.C. (2013). Response surface methodology. Arizona: John Wiley & Sons, Inc.

Neger, M.K. (2002). Literature review on the survival of fecal coliforms in fresh and saline waters, and sediments. Environmental Protection Agency.

Nguyen, D.H., Sebaibi N., Boutouil M., Leleyter L., Baraud, F. (2014). A modified method for the design of pervious concrete mix. Construction and Building Materials Vol 73, 271-282.

Patil, V.R., Gupta, A.K., Desai, D.B. (2011). Use of pervious concrete in construction of pavement for improving their performance. Mechanical and Civil Engineering Vol 54, 2278 – 1684.

Parker, J.K., McIntyre, D., Noble, R.T. (2010). Characterizing fecal contamination in stormwater runoff in coastal North Carolina, USA. Water Research Vol 44, 4186-4194.

Phoo-ngernkham, T., Chindaprasirt, P., Sata, V., Hanjitsuwan, S., Hatanaka S. (2014). The effect of adding nano-SiO_2 and nano-Al_2O_3 on properties of high calcium fly ash geopolymer cured at ambient temperature. Materials & Design Vol 55, 58-65.

Soller, J., Bartrand, T., Ravenscroft, J., Molina, M., Whelan, G., Schoen, M., Ashbolt, N. (2015). Estimated human health reisks from recreational exposures to stormwater runoff containing animal faecal material. Environmental Modelling & Software Vol 72, 21-32.

TDEC. (2014). Tennessee Permanent Stormwater Managment and Design Manual. Tennessee: Tennessee Department of Department of Environment Conservation.

Tkaczewska, E. (2014). Effect of the superplasticizer type on the properties of the fly ash blended cement. Construction and Building Materials Vol 70, 388-393.

Vázquez-Rivera, N.I., Soto-Pérez, L., St John, J.N., Molina-Bas, O.I., Hwang, S.S. (2015). Optimization of pervious concrete containing fly ash and iron oxide nanoparticles and its application for phosphorus removal. Construction and Building Materials Vol 93, 22-28.

Yang, J., Jiang, G. (2003). Experimental study on properties of pervious concrete pavement materials. Cement and Concrete Research Vol 33, 381-386.

Zhong, R., Wille, K. (2015). Material design and characterization of high performance pervious concrete. Construction and Building Materials Vol 98, 51-60.

Appendix

Table A1. Data of pH from rain simulation experiment (Chapter 5)

pH	Phase I				Phase II				Phase III				Phase IV			
Sample	Day 1	Day2	Day 3	Day 4	Day 1	Day2	Day 3	Day 4	Day 1	Day2	Day 3	Day 4	Day 1	Day2	Day 3	Day 4
Influent	7.77	8.33	8.18	8.31	7.30	7.36	7.29	7.31	NO FC				7.51	7.34	7.44	7.39
Influent 2	-	-	-	-	7.17	7.10	7.32	7.07					7.08	7.04	6.95	7.09
Opt 1	8.42	8.36	8.42	8.01	7.49	7.50	7.50	7.55					7.58	7.45	7.36	7.42
Opt 2	8.56	8.57	8.55	8.20	7.61	7.65	7.63	7.46					7.63	7.57	7.43	7.54
Opt 3	8.35	8.49	8.49	8.54	7.74	7.70	7.67	7.35					7.62	7.62	7.55	7.59
Ctrl	8.52	8.48	8.46	8.50	7.86	7.79	7.76	7.63					7.69	7.70	7.63	7.66
Opt 1 B	7.72	7.42	8.08	7.88	7.23	7.27	7.37	7.31					7.27	7.41	7.37	7.32
Opt 2 B	7.92	7.82	8.13	8.02	7.33	7.36	7.44	7.35					7.31	7.29	7.32	7.34
Opt 3 B	8.03	7.99	8.08	8.01	7.42	7.40	7.49	7.42					7.43	7.33	7.36	7.37
Ctrl B	8.12	8.08	8.11	8.02	7.51	7.21	7.51	7.37					7.45	7.39	7.42	7.44

pH	Phase I				Phase II				Phase III				Phase IV			
Sample	Day 1	Day2	Day 3	Day 4	Day 1	Day2	Day 3	Day 4	Day 1	Day2	Day 3	Day 4	Day 1	Day2	Day 3	Day 4
Influent	7.38	8.05	8.07	8.13	7.77	7.82	8.08	7.98	NO FC				8.07	8.12	7.89	7.93
Influent 4	-	-	-	-	7.62	7.16	7.35	7.43					7.34	7.24	7.28	7.28
Opt 4	8.91	9.84	9.51	9.46	9.30	9.71	8.92	8.75					8.68	8.50	8.95	8.67
Opt 5	11.53	11.67	11.52	11.48	11.11	11.20	10.51	10.26					10.07	10.02	10.18	10.43
Opt 4 B	9.01	9.15	9.12	8.97	8.93	9.04	8.69	8.53					8.42	8.43	8.52	8.31
Opt 5 B	11.53	11.52	11.59	11.68	11.05	11.49	10.54	10.65					9.77	10.01	9.94	10.17

Table A2. Data of turbidity from rain simulation experiment (Chapter 5)

Turbidity	Phase I				Phase II				Phase III				Phase IV			
Sample	Day 1	Day2	Day 3	Day 4	Day 1	Day2	Day 3	Day 4	Day 1	Day2	Day 3	Day 4	Day 1	Day2	Day 3	Day 4
Influent	1.49	0.65	1.10	0.39	1.62	3.86	1.15	0.40	NO FC				0.28	5.91	2.02	0.19
Influent 2	-	-	-	-	1.19	1.18	1.41	1.12					1.18	1.40	1.90	1.67
Opt 1	10.83	7.81	8.51	6.67	4.54	7.26	4.47	2.68					3.59	6.91	4.23	2.46
Opt 2	10.18	7.36	6.67	4.56	4.47	4.54	3.58	2.36					2.26	4.03	4.88	2.93
Opt 3	5.41	6.35	4.36	4.66	5.83	4.98	4.80	2.61					2.31	5.32	4.51	2.83
Ctrl	5.79	9.72	3.12	2.48	2.99	4.55	3.35	7.38					2.95	4.80	3.84	1.79
Opt 1 B	2.65	2.09	1.17	0.66	1.13	1.76	1.08	0.61					1.19	1.41	1.84	0.78
Opt 2 B	2.61	1.57	1.01	0.38	0.91	1.46	0.95	0.54					0.74	1.65	1.66	0.82
Opt 3 B	1.81	1.02	0.55	0.51	1.07	1.18	0.71	0.74					0.80	1.30	1.58	0.91
Ctrl B	2.28	0.79	1.21	0.57	1.30	1.50	1.01	0.75					1.22	1.18	1.74	0.63

Turbiduty	Phase I				Phase II				Phase III				Phase IV			
Sample	Day 1	Day2	Day 3	Day 4	Day 1	Day2	Day 3	Day 4	Day 1	Day2	Day 3	Day 4	Day 1	Day2	Day 3	Day 4
Influent	0.15	1.93	2.13	0.99	3.00	0.82	4.75	0.19	NO FC				2.32	1.91	1.00	0.79
Influent 4	-	-	-	-	0.72	2.09	1.02	0.95					1.47	1.26	1.27	1.70
Opt 4	5.88	3.20	3.98	1.64	4.84	2.75	4.63	2.39					2.26	3.11	1.79	2.58
Opt 5	21.03	23.40	9.47	11.90	7.55	6.80	6.59	5.17					3.24	3.93	3.53	3.85
Opt 4 B	1.44	0.97	0.93	0.69	1.22	0.77	1.34	0.50					0.64	0.95	0.51	0.54
Opt 5 B	2.27	2.80	2.10	2.70	2.06	2.02	2.21	1.91					1.04	1.09	1.01	1.53

Table A3. Data of nitrate from rain simulation experiment (Chapter 5)

Nitrate	Phase I				Phase II				Phase III				Phase IV			
Sample	Day 1	Day2	Day 3	Day 4	Day 1	Day2	Day 3	Day 4	Day 1	Day2	Day 3	Day 4	Day 1	Day2	Day 3	Day 4
Influent	0.23	0.22	0.19	0.18	0.31	0.31	0.37	-0.02					0.11	0.40	0.05	0.28
Influent 2	-	-	-	-	3.96	3.52	5.61	2.81					0.84	0.17	3.25	1.04
Opt 1	0.23	0.22	0.20	0.18	0.57	-0.02	0.66	0.15					0.23	0.04	0.08	0.54
Opt 2	0.22	0.22	0.20	0.18	0.14	-0.03	0.00	1.09					0.12	0.04	0.88	0.55
Opt 3	0.23	0.22	0.20	0.18	0.66	0.00	0.28	0.28					0.62	0.45	0.09	0.01
Ctrl	0.22	0.22	0.20	0.16	0.63	0.58	0.17	0.21	NO FC				0.06	-0.01	0.09	0.52
Opt 1 B	0.29	0.26	0.22	0.19	0.57	0.17	0.32	0.19					0.52	0.59	1.03	0.78
Opt 2 B	0.26	0.24	0.21	0.18	0.14	0.60	0.08	0.24					0.52	0.67	1.15	0.64
Opt 3 B	0.26	0.25	0.21	0.18	0.59	0.02	0.02	0.56					0.04	0.08	1.17	0.68
Ctrl B	0.28	0.00	0.22	0.19	0.75	0.29	0.82	0.27					1.06	0.66	0.14	0.64

Nitrate	Phase I				Phase II				Phase III				Phase IV			
Sample	Day 1	Day2	Day 3	Day 4	Day 1	Day2	Day 3	Day 4	Day 1	Day2	Day 3	Day 4	Day 1	Day2	Day 3	Day 4
Influent	0.28	0.37	0.41	0.46	0.42	0.35	0.54	0.47					1.92	1.87	1.94	2.01
Influent 4	-	-	-	-	5.02	1.51	1.93	2.52					3.26	4.86	5.25	5.06
Opt 4	0.39	-0.01	0.40	0.63	0.97	0.46	0.70	0.72	NO FC				2.13	2.29	2.39	2.22
Opt 5	0.04	0.41	0.39	0.39	0.78	0.52	0.74	0.64					1.99	2.25	2.24	2.84
Opt 4 B	0.42	0.37	0.01	0.38	0.72	0.55	0.56	0.61					2.41	2.34	2.45	2.84
Opt 5 B	0.31	0.29		0.44	0.90	0.62	0.67	0.68					2.14	2.21	2.25	2.51

Table A4. Data of TOC from rain simulation experiment (Chapter 5)

TOC	Phase I				Phase II				Phase III				Phase IV			
Sample	Day 1	Day2	Day 3	Day 4	Day 1	Day2	Day 3	Day 4	Day 1	Day2	Day 3	Day 4	Day 1	Day2	Day 3	Day 4
Influent	1.37	1.16	0.96	0.98	1.61	2.11	1.97	1.28	NO FC				1.13	1.86	3.44	1.41
Influent 2	-	-	-	-	3.97	3.80	4.48	3.68					3.08	4.19	4.61	4.16
Opt 1	1.36	1.84	1.23	1.12	2.24	2.72	4.12	2.27					2.28	2.90	4.40	2.21
Opt 2	1.49	1.90	1.30	1.14	2.10	2.90	3.02	2.21					1.85	2.60	4.08	2.76
Opt 3	1.73	2.01	1.50	1.16	2.31	2.72	3.06	2.26					2.22	2.58	4.01	2.08
Ctrl	1.95	1.90	1.33	1.34	2.39	2.81	2.60	3.13					3.70	2.92	3.94	3.75
Opt 1 B	1.85	1.98	1.36	1.23	2.46	2.96	4.07	4.32					2.34	3.03	5.62	3.33
Opt 2 B	1.67	1.67	1.48	1.18	2.31	3.91	3.37	2.44					2.20	3.31	4.12	2.54
Opt 3 B	1.72	1.81	1.51	1.02	2.43	2.86	4.41	3.15					2.70	3.59	4.19	2.73
Ctrl B	1.76	1.75	1.50	1.21	2.67	2.91	3.18	5.22					3.20	3.22	4.34	3.68

TOC	Phase I				Phase II				Phase III				Phase IV			
Sample	Day 1	Day2	Day 3	Day 4	Day 1	Day2	Day 3	Day 4	Day 1	Day2	Day 3	Day 4	Day 1	Day2	Day 3	Day 4
Influent	1.32	1.86	1.68	1.51	1.86	2.03	1.26	1.29	NO FC				1.87	0.97	1.56	1.88
Influent 4	-	-	-	-	0.05	4.77	2.81	3.28					3.63	3.80	3.61	3.63
Opt 4	1.64	1.81	2.11	1.65	3.08	2.78	2.39	2.26					3.55	2.05	2.51	2.99
Opt 5	3.81	2.32	2.34	2.12	2.97	3.53	3.30	2.19					3.01	3.76	2.84	2.40
Opt 4 B	2.54	2.45	2.35	1.99	3.06	2.95	2.22	1.83					2.40	2.59	2.24	4.09
Opt 5 B	3.62	3.80	3.14	2.72	4.19	3.65	3.12	2.55					12.01	6.56	4.50	2.69

Table A5. Data of pH from rain simulation experiment (Chapter 6)

pH	Phase I				Phase II				Phase III				Phase IV			
Sample	Day 1	Day2	Day 3	Day 4	Day 1	Day2	Day 3	Day 4	Day 1	Day2	Day 3	Day 4	Day 1	Day2	Day 3	Day 4
Influent 1	8.47	8.51	8.52	7.81	8.52	8.37	8.82	9.01	NO FC				8.04	8.10	7.93	8.32
Influent 2	-	-	-	-	7.84	7.94	8.27	8.13					7.51	7.81	7.56	8.05
OPT 1A	9.87	9.50	9.45	8.86	9.24	8.98	8.20	8.55					9.21	8.59	9.00	9.04
OPT 1B	9.61	9.52	9.36	9.50	9.15	9.22	8.82	9.08					8.91	9.34	9.12	9.34
OPT 2A	9.08	9.07	8.89	8.94	8.65	8.77	8.70	8.75					8.71	9.15	8.96	8.95
OPT 2B	9.15	9.03	8.93	9.06	8.83	8.85	8.67	8.89					8.69	8.93	8.83	8.93
OPT 3A	9.81	9.26	8.90	9.30	8.94	9.00	9.10	8.97					8.70	9.15	8.97	8.97
OPT 3B	9.32	9.29	9.05	9.16	8.75	8.97	8.87	8.84					8.84	9.08	8.83	8.93
OPT 4A	11.34	11.33	11.38	11.33	11.11	10.90	10.80	10.77					10.69	10.82	10.85	10.70
OPT 4B	11.17	11.41	11.26	10.59	11.13	10.90	10.85	10.61					10.58	10.73	10.62	10.55

Table A6. Data of turbidity from rain simulation experiment (Chapter 6)

Tubidity	Phase I				Phase II				Phase III				Phase IV			
Sample	Day 1	Day2	Day 3	Day 4	Day 1	Day2	Day 3	Day 4	Day 1	Day2	Day 3	Day 4	Day 1	Day2	Day 3	Day 4
Influent 1	0.28	4.51	0.57	0.48	0.28	0.13	0.33	0.14	NO FC				0.09	0.15	0.48	0.22
Influent 2	-	-	-	-	0.98	0.58	0.67	0.82					2.42	1.18	0.92	0.58
OPT 1A	1.34	2.96	1.37	0.45	0.75	0.38	0.28	0.67					0.39	0.40	0.63	0.61
OPT 1B	2.22	3.43	1.45	0.75	0.90	1.98	0.79	0.68					1.11	0.62	0.67	0.48
OPT 2A	1.57	2.85	1.16	0.57	4.32	1.27	0.56	0.30					0.44	0.30	0.57	0.35
OPT 2B	0.94	4.03	1.03	0.57	0.46	0.32	0.44	0.25					1.11	0.27	0.64	0.31
OPT 3A	1.72	3.13	1.17	0.70	0.36	0.86	0.44	0.50					0.62	0.22	0.66	0.23
OPT 3B	1.66	3.63	1.28	0.71	0.46	0.69	0.79	0.61					0.61	0.35	0.65	0.33
OPT 4A	4.27	9.17	2.81	5.38	1.47	1.57	1.59	1.11					0.86	1.83	1.42	1.53
OPT 4B	3.83	5.85	5.10	2.20	10.04	1.03	1.56	0.98					0.83	0.95	1.47	0.53

Table A7. Data of nitrate from rain simulation experiment (Chapter 6)

Nitrate	Phase I				Phase II				Phase III				Phase IV			
Sample	Day 1	Day2	Day 3	Day 4	Day 1	Day2	Day 3	Day 4	Day 1	Day2	Day 3	Day 4	Day 1	Day2	Day 3	Day 4
Influent 1	1.83	1.81	1.81	1.80	1.86	1.81	1.78	1.74					1.74	1.73	1.61	1.68
Influent 2	-	-	-	-	11.41	4.09	11.25	2.98					2.45	2.54	6.36	6.34
OPT 1A	1.84	1.82	1.80	1.77	2.62	1.91	2.53	2.24					1.79	1.73	1.76	2.38
OPT 1B	1.84	1.82	1.80	1.78	2.83	2.29	2.41	1.79					1.83	1.75	1.92	1.92
OPT 2A	1.86	1.82	1.82	1.77	2.43	2.25	2.94	2.08					1.81	1.73	1.78	1.91
OPT 2B	1.85	1.82	1.80	1.79	2.89	2.29	2.52	1.84	NO FC				1.77	1.74	1.97	2.14
OPT 3A	1.86	1.82	1.81	1.78	2.14	2.05	2.41	1.79					1.79	1.73	2.43	1.83
OPT 3B	1.85	1.81	1.81	1.79	4.35	2.26	2.31	1.77					1.81	1.74	2.14	1.82
OPT 4A	1.95	1.88	1.87	1.86	3.24	2.37	2.12	1.83					1.80	1.79	1.89	2.01
OPT 4B	1.93	1.88	1.87	1.84	3.09	2.09	2.57	1.92					1.81	1.77	1.77	2.13

Table A8. Data of phosphate from rain simulation experiment (Chapter 6)

Phosphate	Phase I				Phase II				Phase III				Phase IV			
Sample	Day 1	Day2	Day 3	Day 4	Day 1	Day2	Day 3	Day 4	Day 1	Day2	Day 3	Day 4	Day 1	Day2	Day 3	Day 4
Influent 1	0.00	0.00	0.00	0.00	0.00	0.00	0.00	0.00	NO FC				0.00	0.00	0.00	0.00
Influent 2	-	-	-	-	2.22	2.69	0.00	3.78					13.41	12.84	10.59	10.59
OPT 1A	0.00	0.00	0.00	0.00	0.00	0.00	0.00	0.00					2.19	2.40	2.57	2.74
OPT 1B	0.00	0.00	0.00	0.00	0.00	0.00	0.00	0.00					2.23	2.09	2.24	2.34
OPT 2A	0.00	0.00	0.00	0.00	0.00	1.98	2.08	2.06					2.51	2.30	2.10	2.21
OPT 2B	0.00	0.00	0.00	0.00	0.00	1.99	0.00	0.00					2.15	2.11	2.25	2.61
OPT 3A	0.00	0.00	0.00	0.00	0.00	0.00	0.00	0.00					2.09	2.26	3.07	2.18
OPT 3B	0.00	0.00	0.00	0.00	0.00	0.00	0.00	0.00					2.68	2.16	2.65	2.10
OPT 4A	0.00	0.00	0.00	0.00	0.00	2.01	0.00	0.00					2.13	2.25	2.09	2.27
OPT 4B	0.00	0.00	0.00	0.00	0.00	0.00	0.00	1.98					2.01	2.15	2.05	2.25